The mouse dorsal peduncular cortex encodes fear memory

Rodrigo Campos-Cardoso[1*], Zephyr R. Desa[1,2*], Brianna L. Fitzgerald[1,2], Alana Moore[1], Jace Duhon[1], Victoria A. Landar[1], Roger L. Clem[3], and Kirstie A. Cummings[1#]

[1] Department of Neurobiology, Heersink School of Medicine, University of Alabama at Birmingham, Birmingham, AL, USA

[2] Graduate Biomedical Science Program, University of Alabama at Birmingham, Birmingham, AL, USA

[3] Department of Neuroscience, Friedman Brain Institute, Icahn School of Medicine at Mount Sinai, New York, NY, USA

[*] these authors contributed equally

[#] Correspondence should be addressed to Kirstie A. Cummings, PhD; email: kac3@uab.edu

Abstract

The rodent medial prefrontal cortex (mPFC) is a locus for both the promotion and suppression (e.g. extinction) of fear and is composed of four anatomically distinct subregions, including anterior cingulate 1 (Cg1), prelimbic (PL), infralimbic (IL), and the dorsal peduncular (DP) cortex. A vast majority of studies have focused on Cg1, PL, and IL. The Cg1 and PL have been implicated in the promotion of fear, while the IL has been linked to a role in the suppression, or extinction, of fear. Due to its anatomical location ventral to IL, the DP has been hypothesized to function as a fear-suppressing brain region however, no studies have explicitly tested its role in this function or in the regulation of memory generally. Here, we provide evidence that the DP paradoxically functions as a cued fear-encoding brain region and plays little to no role in fear memory extinction. By using a combination of cFos immunohistochemistry, whole-cell brain slice electrophysiology, fiber photometry, and activity-dependent neural tagging, we demonstrate that DP neurons exhibit learning-related plasticity, acquire cue-associated activity across learning and memory retrieval, and that DP neurons activated by learning are preferentially reactivated upon fear memory retrieval. Further, optogenetic activation and silencing of fear learning-related DP neural ensembles drives the promotion and suppression of freezing, respectively. Overall, these data suggest that the DP plays a novel and unexpected role in fear memory encoding. More broadly, our results reveal new principles of organization across the dorsoventral axis of the mPFC.

Introduction

Several studies have pointed towards the rodent medial prefrontal cortex (mPFC) as a locus important for both the promotion and suppression of fear. The mPFC is comprised of four anatomically and functionally distinct subregions including the anterior cingulate 1 (Cg1), prelimbic cortex (PL), infralimbic cortex (IL), and the dorsal peduncular cortex (DP). Numerous studies have largely ascribed the dichotomous role for the mPFC to PL and IL subdivisions, which play a role in the promotion and suppression of fear, respectively [1–5]. Similar to the PL, Cg1 has also been implicated in signaling fear [6,7]. In contrast, the specific role of the DP has largely been overlooked. The roles for Cg1 and PL in the promotion of fear and IL in the suppression of fear have led to the proposal that mPFC exhibits an organized functional architecture across the dorsoventral axis. Therefore, due to its anatomical location ventral to IL, some have hypothesized that DP also functions to suppress fear [8]. Despite this, the role that DP might play in fear suppression or some other aspect of memory has not been tested.

In contrast to its proposed role in safety learning, several studies suggest a role for the DP in processing aversive stimuli. Following social defeat stress, the DP, along with the region immediately ventral, the dorsal tenia tecta (DTT), have been implicated in driving physiological sympathetic responses, including thermoregulation and cardiac responses [9–11]. Moreover, a recent study has also implicated the DP/DTT in driving anxiety-like behaviors [12]. Given the central role for autonomic responses in fear, we hypothesized that the DP may be playing a role in fear memory processes rather than in extinction. Indeed, in humans, the ventromedial prefrontal cortex has been implicated both in the inhibition and expression of fear [13–16]. Nevertheless, despite this, the role for the DP in fear memory processing is largely unknown.

Here, we use a combination of whole-cell brain slice electrophysiology, activity- dependent neural tagging, immunohistochemistry, fiber photometry calcium imaging, and *in vivo* optogenetics to probe the role for the DP in the regulation of fear memory. We surprisingly found that rather than suppressing fear, neural ensembles in DP paradoxically function to encode fear memory and drive defensive behaviors. Our results provide a new role for the DP in fear memory encoding and fundamentally upend our understanding of the functional organization of the mPFC.

Results

DP is activated in response to fear- but not extinction-related stimuli.

To test whether the DP is involved in fear or extinction memory processes, we performed cFos immunohistochemical staining following exposure to three different behavioral paradigms. The first group of mice were subjected to tones only followed by a tone re-exposure test 24 hours later (**Figure 1A; Supplementary Figure 1**). The second group consisted of mice that were subjected to fear conditioning, which consisted of paired presentations of conditioned stimuli (CS; auditory tone) and unconditioned stimuli (US; foot shock) followed by a CS-evoked fear memory retrieval test 24 hours later (**Figure 1B; Supplementary Figure 1**). The third group consisted of mice subjected to paired fear conditioning followed by two consecutive days of CS extinction training. Animals from this group were then subjected to an extinction memory retrieval test 24 hours after the second day of extinction training (**Figure 1C; Supplementary Figure 1**). At 90 minutes after tone re-exposure or CS-evoked fear or extinction memory retrieval, mice were subjected to transcardial perfusion and brains were processed for cFos immunohistochemistry. cFos+ puncta were then quantified across the Cg1, PL, IL, and DP subregions of mPFC in mice from each behavioral group (**Figure 1D**). No differences in the density of cFos+ cells were observed across behavior groups in either the Cg1 or PL, consistent with our previous observations in the PL [17] (**Figure 1E-F**). In the IL, we observed a significant increase in the density of cFos+ cells in the extinction group compared to tones-only or fear conditioned mice (**Figure 1G**). This result is consistent with the role for the IL in extinction memory processing [5]. Compared to tones-only mice, those that were subjected to conditioning and fear memory retrieval exhibited a significantly higher density of cFos+ cells in the DP (**Figure 1H**). In contrast, mice subjected to extinction training exhibited a significantly lower density of cFos+ cells in the DP compared to conditioned mice. These results suggest that rather than participating in extinction memory processing as was hypothesized previously, the DP may paradoxically be involved in fear-related memory processing.

DP principal neurons exhibit fear learning-related plasticity.

A hallmark of memory encoding is thought to be the expression of learning-related plasticity. We therefore sought to determine whether fear conditioning results in experience-dependent changes in DP neuron synaptic transmission. We performed whole-cell electrophysiological recordings in DP principal neurons (PNs) in acute brain slices prepared from wild-type mice. Prior to recording, mice were subjected to paired or unpaired fear conditioning (**Figure 2A; Supplementary Figure 2**). An additional group of mice were left trained and were only home cage-experienced. Acute brain slices were prepared 24 hours after behavioral training and spontaneous excitatory (EPSCs) and inhibitory (IPSCs) postsynaptic currents were recorded from DP PNs. Mice that were subjected to paired fear conditioning exhibited a higher frequency of spontaneous EPSCs onto DP PNs as compared to unpaired and naive control mice (**Figure 2B-C**). No group-dependent

differences in spontaneous EPSC amplitude or IPSC frequency or amplitude were observed (**Figure 2D-E**). These results suggest that paired fear conditioning drives the potentiation of excitatory transmission onto DP PNs.

DP neurons exhibit CS-related activity during conditioning and memory retrieval.

The previous experiments lead to the observation that paired fear conditioning leads to strengthening of excitatory inputs onto DP PNs. These results may point towards a role for DP in cue-related fear memory processing. To test this possibility, we performed fiber photometry calcium imaging in the DP of mice undergoing fear conditioning and memory retrieval. Wild-type mice received unilateral infusions of GCaMP8f in DP as well as angled imaging fiber implantation immediately dorsolateral to the DP (**Figure 3A-B; Supplementary Figure 3**). We continuously recorded calcium associated transients from DP neurons during a pre-conditioning CS exposure test, during paired fear conditioning, and during CS-evoked fear memory retrieval. During fear conditioning, we observed a trial-dependent increase in cue-related activity, consistent with DP neurons having the ability to track and potentially encode information about the cue (**Figure 3C**). At 24 hours after conditioning, mice were placed in a neutral context and subjected to a cue-evoked fear memory retrieval test. Consistent with the idea that DP encodes cue-related information, we observed strong cue-elicited calcium signals. These signals were significantly larger than those recorded from the same mice in a preconditioning tone exposure test (**Figure 3D**). These results suggest that the DP tracks and encodes cue-related information during fear conditioning and memory retrieval.

We also tested whether DP neurons may participate in extinction memory processing, as was previously proposed for this region [8]. To test this possibility, 24 hours following the fear memory retrieval test, mice were subjected to two consecutive days of cue extinction training followed by an extinction memory retrieval test 24 hours later. In contrast to the signals observed during fear memory retrieval, we did not observe significant CS-related activity during cue presentation in the extinction retrieval test (**Figure 3C-D**). Instead, the calcium-associated activity returned to baseline-like levels that were not different from those recorded in the preconditioning tone-exposure test. Taken together, these results further support the idea that DP is involved in encoding cued fear memory, but does not appear to participate in extinction memory processes.

DP neurons are activated by fear conditioning and reactivated in response to CS-evoked fear memory retrieval.

The previous experiment revealed that DP neurons are activated both during fear memory acquisition and memory retrieval. However, it remained unclear whether the same or different DP neurons are activated during learning and retrieval, a pattern of activity that is thought to be a hallmark of memory encoding neurons. Towards this goal, we employed an activity-dependent neural tagging strategy that we previously used to tag fear-activated neurons [17]. This strategy entails the use of a vector that allows for the activity-dependent expression of a 4-hydroxytamoxifen- (4-OHT) inducible Cre recombinase under the control of the synthetic enhanced synaptic activity-responsive element (ESARE-ERCreER) promotor [18]. A vector encoding ESARE-ERCreER was infused in the the medial prefrontal cortex along with additional vectors encoding a Cre-dependent enhanced yellow fluorescent protein (DIO-eYFP) as well as an mCherry under the control of the human synapsin promotor (hSyn-mCherry) (**Figure 4A**). After 4 weeks, mice were subjected to either paired fear conditioning or to tones only (**Supplementary Figure 4**). Immediately after training, mice received intraperitoneal (IP) injections of either 4-OHT or vehicle. After two weeks, which is required for recombination and protein expression, mice were subjected to a CS-evoked fear memory retrieval test or tone re-exposure test in a neutral context after which they were transcardially perfused. Brain tissue was then processed for cFos immunohistochemistry (**Figure 4B**).

We observed that there were significantly more eYFP+ neurons in the DP of 4-OHT-injected conditioned mice compared to vehicle-injected conditioned mice or 4-OHT- or vehicle-injected tone-exposed mice (**Figure 4C**). While cFos-levels were comparable across groups (**Figure 4D**), there was an enrichment in

147 the number of tagged neurons that were positive for cFos in the 4-OHT-injected conditioned group compared
148 to those injected with vehicle or to vehicle- and 4-OHT-injected tones-only mice (**Figure 4E**). Comparisons of
149 the proportion of cFos-positive tagged neurons revealed that 4-OHT-injected conditioned mice had significantly
150 higher levels (~40%) of fear retrieval-reactivated learning-tagged DP neurons compared to any other group
151 (**Figure 4F**). These results reveal that ensembles of DP neurons exhibit activity patterns consistent with a role
152 in fear memory encoding.
153 The results from our cFos (**Figure 1**) and fiber photometry experiments (**Figure 3**) suggested that DP
154 neurons are activated in response to fear conditioning and cue-evoked fear memory retrieval, but not following
155 extinction. To further test whether DP may be playing a role in extinction, we performed activity-dependent
156 neural tagging following extinction training (**Supplementary Figure 5**). Following vector cocktail infusion in the
157 IL and DP, mice were subjected to paired fear conditioning and three consecutive days of cue extinction
158 training. Following the third extinction trial, mice received IP injections of either vehicle or 4-OHT. Two weeks
159 later, brains were processed for immunohistochemistry. Consistent with our previous results, we only observed
160 a small fraction of the total number of tagged neurons in the DP, and there was no difference in the number of
161 tagged neurons in DP in the vehicle compared to the 4-OHT group. Importantly, a vast majority of tagged
162 neurons instead resided in the IL, which has been implicated in extinction. Consistent with its role in extinction,
163 there were significantly more tagged neurons in the IL of 4-OHT injected mice compared to those injected with
164 vehicle. These results are also consistent with cFos immunohistochemistry results suggesting that cells in the
165 IL but not DP are activated following extinction training (**Figure 1G-H**). Overall, these results provide additional
166 evidence suggesting that the DP is involved in fear- but not extinction-related processes.
167 We additionally performed neural tagging in the DP following unpaired conditioning, in which mice were
168 subjected to both the CS and US but in an explicitly unpaired manner (**Supplementary Figure 6**). Immediately
169 after US delivery, mice received IP injections of either vehicle or 4-OHT. Two weeks after training, mice were
170 subjected to a CS-evoked fear memory retrieval test and cFos immunohistochemistry was performed.
171 Comparisons of the proportion of cFos+ eYFP neurons in vehicle versus 4-OHT-injected mice revealed no
172 significant group differences. These results further support the idea that cue fear learning-tagged DP neurons
173 represent a distinct learning-related population, rather than an ensemble activated by stress, contextual
174 elements, or some other stimulus.
175
176 **Activity of fear-tagged DP neurons is necessary and sufficient for fear memory expression.**
177 Given that learning-activated DP neurons are reactivated following CS-evoked fear memory retrieval,
178 we next sought to test whether the activity of fear-tagged DP neurons can modulate fear memory expression.
179 Towards this goal, we infused vectors encoding ESARE-ERCreER, Cre-dependent eYFP-tagged
180 channelrhodopsin (DIO-ChR2-eYFP) or green fluorescent protein-tagged archaerhodopsin (FLEX-Arch-GFP),
181 and hSyn-mCherry bilaterally into the DP of wild-type mice (**Figure 5A**). Following vector infusion, optic fibers
182 were implanted bilaterally and directed at the DP (**Supplementary Figure 7**). After 4 weeks, mice were
183 subjected to paired fear conditioning and immediately injected with vehicle or 4-OHT. After 2 weeks, mice were
184 subjected to a fear memory retrieval test in a neutral context and laser stimulation-dependent alterations in
185 freezing were assessed. In 4-OHT-injected mice expressing ChR2, optogenetic activation (473 nm, 20 Hz, 5
186 ms pulses, 20 s epochs) of fear-related DP neurons led to a significant increase in freezing over baseline
187 (**Figure 5B**). Conversely, optogenetic silencing (532 nm, solid light, 20 s epochs) of fear-tagged DP neurons
188 resulted in a reduction in CS-evoked freezing compared to CS presentation in the absence of optogenetic
189 silencing (**Figure 5C**). Open field test during which optogenetic activation and silencing was performed
190 revealed that there was no significant light-dependent effect on either locomotion or on anxiety-like behaviors
191 (**Supplementary Figure 8**). Importantly, recordings from brain slices containing fear-tagged DP neurons
192 expressing Arch-GFP or ChR2-eYFP revealed that the *in vivo* optogenetic manipulation procedures used result
193 in reliable neural silencing or activation, respectively (**Supplementary Figure 9**). Overall, these results suggest
194 that the activity of fear-tagged DP neurons is both necessary and sufficient for fear memory expression.
195

Discussion

Here, we reveal that the DP is critically involved in fear memory encoding and expression. We found that auditory fear conditioning but not extinction training drives activity of DP neurons. Moreover, fear conditioning potentiates glutamatergic transmission onto DP PNs compared to naive and unpaired littermate controls. By using fiber photometry recordings, we observed that DP neurons acquire CS-related activity during memory acquisition and that this activity persists during subsequent fear memory retrieval, but is lost after extinction training. Activity-dependent neural tagging following memory acquisition combined with cFos immunohistochemistry after retrieval indicated that ensembles of DP neurons are activated by learning and reactivated following memory retrieval. Finally, optogenetic activation of learning-tagged DP neurons induces fear memory expression whereas silencing significantly suppressed cue-evoked freezing. Taken together, our results point towards an unexpected role for the DP in fear memory processing - an observation that is at odds with its proposed role in extinction [8].

The rodent vmPFC is most well-known for its role in memory extinction. In particular, lesion experiments [19–21], *in vivo* electrophysiological recordings and electrical stimulation [22,23], pharmacological microinfusion experiments [24], and *in vivo* optogenetic manipulations [5] have pointed towards a role for vmPFC in extinction memory processing, with a vast majority of this role attributed to the IL. However, some additional studies have provided conflicting results regarding this role. For example, *in vivo* pharmacological inhibition of vmPFC has paradoxically been shown to reduce the expression of conditioned fear [25]. Moreover, additional lesion studies found that vmPFC lesions had no effect on extinction memory acquisition or retrieval [26,27]. These conflicting findings are also reflected in the human literature where studies have implicated the vmPFC in extinction [1,13,14] while other studies have suggested vmPFC activity contributes to the pathology of post-traumatic stress disorder [15,16]. While the conflicting results in rodents can potentially be explained by compensatory mechanisms or differences in experimental execution, one additional possibility may be due to differences in the lesion/ infusion locus within vmPFC. The results of our current study that implicate the DP in fear but not extinction memory processes may potentially account for the conflicting findings in the field.

A recent study revealed sexual dimorphic activity profiles in the DP following auditory fear conditioning, where female mice exhibited significantly higher levels of conditioning-induced cFos expression compared to males [28]. While most of our experiments are not sufficiently powered to perform rigorous sex differences analyses, our results do not point toward any gross differences in DP activity in male and female mice. Whether conditioning engages distinct cell types or circuits within the DP of male and female mice remains to be an important area for future investigation.

As the role for DP in fear memory encoding and retrieval as well as in processing other emotional stimuli continues to be investigated, additional questions remain to be answered in future studies. One such question is why might both the PL and the DP function to encode fear memory? Are each of these brain regions encoding distinct aspects of the fear memory? Some of these insights may be gained through the systematic investigation of projection pathways that may differentially engage the PL versus the DP. However, no studies exist that explicitly examine the anatomical connectivity of the DP. Functional *in vivo* oscillation measurements across mPFC subregions in anesthetized rats have revealed vast differences in the PL and DP, suggesting that these regions may have unique functions and/or connectivity patterns [29]. Moreover, an anatomical analysis reveals bidirectional connectivity between the PL and DP[30], suggesting that they may convey information to each other during memory encoding. Therefore, it will be important for future studies to reveal the fundamental connectivity of long-range inputs to DP in order to gain insight to these questions. An additional intriguing question is why the IL is located between two fear-promoting brain regions. The PL has been shown to be involved in extinction memory acquisition through dense L5/6 glutamatergic projections to L5/6 IL neurons [31]. Whether and how the DP might engage either the IL or the PL following fear conditioning and/or extinction is an area open for inquiry.

Our results suggest that a relatively sparse ensemble of DP neurons functions to encode fear memory. While we have characterized the functional contributions of this ensemble, several questions remain. First, it remains unknown what neuron type(s) comprise this ensemble and how these distinct cell types contribute to

memory encoding. Our previous work revealed that somatostatin-expressing interneurons (SST-INs) comprise a relatively large part of the fear-activated ensemble in the PL [17]. Whether these or another subset of interneurons are recruited into the DP ensemble remains unknown. Additionally, future studies should focus on revealing the local microcircuit connectivity and plasticity mechanisms that support the recruitment of the DP ensemble. Indeed, our previous work in the PL revealed that there is extensive rebalancing of microcircuit activity that resulted in SST-IN-mediated inhibition of parvalbumin-expressing interneuron (PV-IN) activity, driving the disinhibition of PNs [32]. Whether this circuit organization and plasticity mechanism is conserved in the DP is unknown and should be studied in future work.

Overall, our results provide the first insights to fear memory encoding and expression in the mouse DP. These findings open several new areas of investigation and fundamentally redefine our understanding of the functional landscape within the rodent mPFC.

Methods

Animals. The use of animals in all experimental procedures was approved by the Institutional Animal Care and Use Committee at the Heersink School of Medicine at the University of Alabama at Birmingham. Both male and female mice at the age of postnatal day 42 (P42) were used for stereotaxic surgery and behavioral experiments were then performed at P60-90. Mice used in experiments were the C57Bl/6J genotype (stock no. 000664). Animals were housed in groups of 2-6 with a 12 h light-dark cycle and *ad libitum* access to food and water. Equal numbers of males and females were used for all experimental groups.

Behavioral training paradigms. Auditory fear conditioning was performed by subjecting mice to 6 pairings of a pure auditory tone (CS; 80 dB, 2 kHz, 20 s) with a co-terminating scrambled foot shock (US; 0.7-1.0 mA, 2 s). Unpaired conditioned mice were subjected to 6 CS presentations after which they were returned to their home cage for 15 min and then placed back into the arena during which they received 6 US presentations. Naive mice only experienced the home cage. Tones-exposed mice were placed in the conditioning arena and subjected to 6 CS tones in the absence of the US. For extinction training, 24 hours after paired fear conditioning, mice were placed in a neutral context (context B) consisting of distinct visual, olfactory, and tactile cues and subjected to 20 CS tones. An additional extinction session was performed the next day for a total of 2 consecutive days. For either fear or extinction memory retrieval in cFos, electrophysiological, and calcium imaging experiments (Figures 1, 2, and 3), mice were placed in context B and subjected to presentation of 4 CS tones at 24 hours after either fear conditioning or the second day of extinction training, respectively. Tone re-exposure was performed in context B by presenting animals 4 CS tones at 24 hours after tone exposure. For fear memory retrieval or tones re-exposure following neural tagging (Figures 4 and 5), mice were placed in context B and subjected to presentation of 4 CS tones at 2 weeks (due to limitations of vector expression timeline) after fear conditioning or tone exposure, respectively. Littermates were used for each experiment whenever possible and were randomly distributed across behavior groups in an interleaved fashion.

Immunohistochemistry. Immunohistochemistry was performed for cFos and/or GFP. 90 minutes after the last behavioral test, after deep isoflurane anesthesia was induced, mice were transcardially perfused with phosphate buffered saline (PBS; pH 7.4) followed by 4% paraformaldehyde in PBS (PFA; pH 7.4) before removal of the brains. Brains were then fixed in 4% PFA overnight before sectioning 50 µm coronal slices using a Leica VT1000S vibratome (Leica Biosystems, Deer Park, IL, USA).

Brain sections were blocked with 5% normal goat serum in PBS + 0.3% Tween-20 for one hour at room temperature. Afterwards, slices were incubated at 4° C overnight with rabbit anti-cFos primary antibody (1:1000; Millipore ABE457). The following day, slices were incubated for 2 hours with a secondary anti-rabbit antibody conjugated to Alexa 647 (1:500; Jackson Immunoresearch, 111-605-045) with 5% normal goat serum in PBS + 0.3% Tween-20.

For experiments requiring staining against GFP, slices were then incubated overnight with a chicken anti-GFP primary antibody (1:500; Millipore AB16901) with 5% normal donkey serum in PBS + 0.3% Tween-

20. The next day, slices were incubated with a secondary anti-chicken antibody conjugated to Alexa 488 (1:500; Jackson Immunoresearch, 703-095-155) for 2 hours at room temperature.

Following immunohistochemical staining, slices were mounted with ProLong Gold antifade reagent with DAPI (Life Technologies, Eugene, OR, USA). Imaging was performed using an upright Echo Revolution hybrid microscope (BICO, San Diego, CA, USA). Cell counting for cFos- or/ and GFP-labeled cells was performed with the Cell Counter plug-in through the ImageJ program (NIH, Bethesda, MD, USA). Quantification was performed for either or both cFos+ and GFP+ cells, as well as for overlapping cFos+/GFP+ cells by experimenters blind to experimental conditions and groups.

Whole-cell brain slice electrophysiology. Mice were subjected to paired fear conditioning, unpaired fear conditioning, or were naive. 24 hours after training, mice were used for electrophysiology recordings.

Mice were deeply anesthetized by way of isoflurane administration prior to decapitation. Brain slices containing the mPFC were sectioned at 300 µm on a Leica VT1200S vibratome in chilled carbogen-bubbled low sodium sucrose cutting solution containing (in mM) 210 sucrose, 11 glucose, 26.2 $NaHCO_3$, 2.5 KCl, 1 NaH_2PO_4, 4 $MgCl_2$, 0.5 $CaCl_2$, and 0.5 ascorbate. Slices were then recovered for 45 min in warmed (32° C) carbogen-bubbled normal artificial cerebrospinal fluid containing (in mM) 119 NaCl, 26.2 $NaHCO_3$, 11 glucose, 1 NaH_2PO_4, 2 $MgCl_2$, 2.5 KCl, 2 $CaCl_2$. Slices were kept at room temperature. Whole-cell electrodes (3-4 MΩ) were fabricated from fire polished borosilicate capillaries and filled with internal solution containing (in mM) 120 Cs-methanesulfonate, 10 HEPES, 10 Na-phosphocreatine, 1 QX-314, 8 NaCl, 0.5 EGTA, 4 Mg-ATP, 0.4 Na-ATP (pH 7.25; 290-300 mOsmol). Cells were visualized on an upright microscope equipped with differential interference contrast optics. Principal neurons were identified visually (large pyramidal somas) and electrophysiologically (low membrane resistance (<75 MΩ) and high capacitance (>100 pF). Cells were sampled across superficial and deep layers and pooled.

Excitatory (EPSC) and inhibitory (IPSC) postsynaptic currents were recorded in standard artificial cerebrospinal fluid by clamping cells at -60 mV or 0 mV, respectively. Each EPSC and IPSC recording lasted at least 5 min. Data were sampled at 10 kHz and low-pass-filtered at 3 kHz using Multiclamp 700B amplifier (Molecular Devices, version 2.2.2.2). Data were analyzed in EasyElectrophysiology (version 2.5.1) by experimenters blind to experimental groups. Access resistance and leak current were monitored throughout each recording. Recordings that yielded unstable currents (>150 pA leak; >20% change in access resistance) or which did not meet cell type characterization requirements were excluded. Cell exclusion was rare and occurred <2% of the time.

Stereotaxic vector infusion and fiber implantation. AAV2/8-ESARE-ERCreER-PEST was received as a gift from Dr. Harihiko Bito (U. Tokyo) and custom packaged at Boston Children's Hospital Vector Core. AAV1-DIO-eYFP (Cat. No. 27056), AAV8-hSyn-mCherry (Cat. No. 114472), AAV1-hSyn-GCaMP8f (Cat. No. 162376), AAV1-DIO-hChR2(H134R)-eYFP-WPRE (Cat. No. 20298), and AAV1-FLEX-Arch-GFP (Cat. No. 22222) were purchased from Addgene. For all experiments, vector infusions occurred at P42. For activity-dependent tagging quantification experiments (Figure 4; Supplementary Figures 5 and 6), vectors were infused bilaterally in the DP (200 µl; A/P: 1.55; M/L: +/- 0.25; D/V: -3.7) or in DP and IL (400 µl; A/P: 1.55; M/L: +/- 0.25; D/V: -3.7-3.5). Vectors were mixed at a 2 (ESARE-ERCreER-PEST) to 7 (DIO-eYFP) to 1 (hSyn-mCherry) ratio just prior to stereotaxic infusion. For fiber photometry experiments (Figure 3) and *in vivo* optogenetics (Figure 5), vectors were infused unilaterally (fiber photometry) or bilaterally (*in vivo* optogenetics) into the DP (A/P: 1.55; M/L: + and/or - 0.25; D/V: -3.7). For fiber photometry experiments, an imaging fiber (400 µm diameter, 0.48 NA, Doric Lenses) was implanted immediately above the DP (A/P: 1.6; M/L: +/- 1.65; D/V: -3.9; 32° angle). For *in vivo* optogenetic experiments, optic fibers were implanted directed at DP (A/P: +1.6; M/L: +/- 1.65; D/V: -3.8; 32° angle). Vector incubation times were previously determined [17,32] or were determined empirically for this study.

342 **Activity-dependent neural tagging and cFos immunofluorescence.** At 3.5 weeks post vector cocktail
343 infusion, mice were handled for three days consecutively prior to behavior. Mice were subjected either to
344 auditory paired fear conditioning, tones-only, or unpaired fear conditioning. For mice used to tag extinction-
345 related mPFC neural ensembles, animals were subjected to extinction training for 3 consecutive days starting
346 at 24 hours after fear conditioning. Neural tagging was performed through an intraperitoneal (IP) injection of 4-
347 OHT (10 mg/kg) or vehicle solution immediately after the completion of the last day of training, as was done
348 previously [17]. Two weeks after training and activity-dependent tagging, mice were subjected to a fear memory
349 retrieval test in a neutral context (context B). Mice were sacrificed 90 minutes post-retrieval for cFos and GFP
350 immunohistochemistry as described above.
351
352 **Fiber photometry recording and analysis.** Fiber photometry recordings were performed by using a complete
353 system from Tucker-Davis Technologies, as we have done previously [32]. At 4 weeks after vector infusion and
354 imaging fiber implantation, mice were habituated to handling and patch cord tethering for 3 consecutive days.
355 Mice were placed in a neutral arena with white floor and rounded wall inserts (context B) and subjected to 4 CS
356 presentations (CS: 80 dB, 2 kHz, 20 s). 24 h later, mice were subjected to paired fear conditioning in an arena
357 with a metal grid floor and square metal walls (context A). Mice were then subjected to a fear memory retrieval
358 test at 24 h post-conditioning. 24 hours later, mice were subjected to two consecutive days of extinction
359 training in context B. At 24 h post extinction training, mice were subjected to an extinction memory retrieval test
360 in context B. Calcium signals were sampled at 6 kHz and continuously recorded throughout the duration of
361 each behavioral test. Transistor-transistor logic (TTL) signals were generated through MedAssociates software
362 and were used to produce timestamps for the start and stop of each session as well as for CS presentation
363 epochs. Prior to the start of each session, calcium signals were recorded for a duration of 2 min to ensure
364 stable recordings.
365 Data were processed and analyzed using custom-written code from the Tucker-Davis Technologies
366 website as described previously [32]. Briefly, CS-associated activity changes were calculated by normalizing the
367 calcium signal during the 20 s CS presentation to a 20 s baseline period occurring immediately prior to CS
368 onset. The percentage change in fluorescence (%$\Delta F/F$) was calculated by subtracting the peak baseline signal
369 from the peak signal during CS presentation and dividing by the peak baseline signal (%$\Delta F/F = (F_{peak}CS -$
370 $F_{peak}BL)/F_{peak}CS)$). Reported values represent within-animal changes. At the conclusion of experiments, mice
371 were subjected to transcardial perfusion with PBS followed by 4% paraformaldehyde and imaging fiber
372 placement and GCaMP8f expression was assessed. Mice with incorrect fiber placements and/or GCaMP8f
373 expression were excluded from analyses.
374
375 ***In vivo* optogenetics.** At 3.5 weeks after vector infusion and optic fiber implantation, mice were habituated to
376 handling and tethering to patch cords for 3 consecutive days. Mice were subjected to paired fear conditioning
377 and then received intraperitoneal injections of either 4-OHT (10 mg/kg) or vehicle immediately after training
378 and returned to their home cage. After two weeks, mice were subjected to a CS-evoked fear memory retrieval
379 test in a neutral context (context B). Optogenetic activation (473 nm, 20 Hz, 5 ms pulses, 20 s epochs) or
380 silencing (532 nm, solid light, 20 s epochs) was performed in animals expressing ChR2 or Arch, respectively.
381 Light intensities delivered to the brain were measured and calculated prior to each experimental day and
382 ranged from 6-8 mW. Optogenetic manipulations were performed alone or in combination with the CS in an
383 alternating manner (e.g. Baseline: light-on, light-off; CS: CS + light, CS alone, etc) and the order or light
384 presentation was counterbalanced. Each epoch (baseline, light-on; baseline, light-off; CS, light-on; CS, light-
385 off) was repeated twice per animal and the average was reported. Videos were scored by experimenters blind
386 to experimental conditions and groups. At the end of the experiment, mice were subjected to transcardial
387 perfusion and brains were sectioned for immunohistochemical analysis to confirm correct optic fiber placement
388 and vector expression. Mice with incorrect fiber placement and/or viral expression were removed from
389 analyses.
390

Open field test. Mice from the *in vivo* optogenetics experiments (Figure 5) were also subjected to optogenetic stimulation in an open field. The test was 10 minutes in duration, and consisted of alternating and counterbalanced epochs of 1 minute light-on and 1 minute light-off periods. The open field measured 40 cm length x 40 cm width x 40 cm height and tracked movement via infrared beam breaks (MedAssociates, Fairfax, VT). Average distance moved and average percent time spent in the margin space was calculated and reported for each mouse for the light-on/ light-off epochs.

Electrophysiological validation of *in vivo* optogenetic manipulations. To validate the modes of optogenetic manipulation of fear-related DP neurons used *in vivo* (Figure 5), mice that received infusions of vectors encoding ESARE-ERCreER and either DIO-ChR2-eYFP or FLEX-Arch-GFP were subjected to paired fear conditioning and intraperitoneal injection of 4-OHT (10 mg/kg). After 2 weeks, mice were used to prepare brain slices, as described above. DP neurons expressing ChR2 or Arch were targeted in slice via fluorescence. For DP neurons expressing Arch, after achieving whole-cell configuration, slow current was injected to induce spontaneous action potential firing. Green light (532 nm; solid light; 8 mW; 20 sec epochs) was delivered via LED-coupled objectives for a total of 4-5 times per cell. The average firing frequency and magnitude of hyperpolarization was calculated during light off and light on epochs. For DP neurons expressing ChR2, after achieving the whole-cell configuration, pulses of blue light (473 nm; 20 Hz, 5 ms pulses, 20 sec epochs) were delivered via LED-coupled objectives and action potential firing was recorded.

Statistical analysis. Levine's and Shapiro-Wilk tests were performed prior to parametric statistical testing to test whether data exhibited homogeneity of variance and normal distribution, respectively. If either or both conditions were not met, data were subjected to non-parametric statistical analyses. Statistical testing and graph plotting were performed using OriginPro 2019 version 9.6.0.172.

Acknowledgments
These experiments were supported by the National Institute of Mental Health grant no. R00 MH122228 to K.A.C., diversity supplement under R00 MH122228 to B.L.F., Brain and Behavior Research Foundation Young Investigator Award to K.A.C., and Joe W. and Dorothy Dorsett Brown Foundation grant to K.A.C.

Contributions
K.A.C. and R.L.C initiated the project. K.A.C supervised the research. K.A.C, R.C.C, Z.R.D, B.L.F., and R.L.C. designed experiments. K.A.C., R.C.C., Z.R.D., B.L.F., A.M., J.D., and V.A.L. performed the research and data analysis. K.A.C., R.C.C., and Z.R.D. wrote the manuscript.

Figure legends
Figure 1. Fear conditioning drives activation of the DP. Mice were subjected either to (A) 6 tones (2 kHz, 20 s, 80 dB) followed by a tone re-exposure test consisting of 4 tone (2 kHz, 20 s, 80 dB) presentations 24 hours later; (B) paired presentations of a CS (2 kHz, 20 s, 80 dB) and US (2s, 0.7 mA) followed by a fear memory retrieval test consisting of 4 CS presentations (2 kHz, 20 s, 80 dB) 24 hours later; or to (C) paired presentations of a CS (2 kHz, 20 s, 80 dB) and US (2s, 0.7 mA) and 2 consecutive days of extinction training consisting of 20 CS (2 kHz, 20 s, 80 dB) presentations, and an extinction memory retrieval test consisting of 4 CS (2 kHz, 20 s, 80 dB) presentations. 90 minutes after tone re-exposure or fear or extinction memory retrieval, tissue was collected for cFos immunohistochemical analysis. (D) Representative histological images of prefrontal brain sections obtained from mice subjected to tones only, fear conditioning, or fear extinction. Scale = 500 µm. Comparisons of cFos+ puncta density between tones only (n = 5 mice, 10 slices), conditioning (n = 5 mice, 10 slices), and extinction (n = 7 mice, 14 slices) groups in the (E) anterior cingulate cortex 1 (Cg1: $F_{2,14} = 4.08$, $P = 0.04$, one-way ANOVA), (F) prelimbic cortex (PL: $F_{2,14} = 2.23$, $P = 0.14$, one-way ANOVA), (G) infralimbic cortex (IL: $F_{2,14} = 19.34$, $P = 9.4 \times 10^{-4}$, one-way ANOVA), and (H) dorsal peduncular cortex (DP: $X^2 = 9.39$ (2), $P = 0.009$, Kruskal-Wallis ANOVA). *P < 0.05, ***P < 0.001, Tukey's

post-hoc test. Box plots represent the median (center line), mean (square), quartiles, and 10-90% range (whiskers). Open circles represent data points for individual mice.

Figure 2. Fear conditioning drives increased glutamatergic transmission onto DP PNs. (A) Mice were either experienced to their home cage (naïve) or subjected to unpaired or paired presentations of a CS (2 kHz, 20 s, 80 dB) and US (2s, 1 mA). Whole-cell recordings were performed 24 hours after training. (B) Representative spontaneous excitatory postsynaptic current (EPSC) recordings in DP PNs from brain slices prepared from naïve (8 slices from 4 mice), unpaired (5 slices from 3 mice), and paired (8 slices from 4 mice) mice. (C) Quantification of the EPSC amplitude and interevent interval for naïve, unpaired, and paired groups. Amplitude: $F_{2,35} = 1.67$, $P = 0.2$, one-way ANOVA; naïve = 14 cells; unpaired = 10 cells; paired = 14 cells. Interevent interval: $X^2 = 14.32$ (2), $P = 7.77 \times 10^{-4}$, Kruskal-Wallis ANOVA; naïve = 14 cells; unpaired = 10 cells; paired = 14 cells. (D) Representative spontaneous inhibitory postsynaptic current (IPSC) recordings in DP PNs from brain slices prepared from naïve, unpaired, and paired mice. (E) Quantification of the IPSC amplitude and interevent interval for naïve, unpaired, and paired groups. Amplitude: $F_{2,32} = 0.084$, $P = 0.92$, one-way ANOVA; naïve = 13 cells; unpaired = 10 cells; paired = 12 cells. Interevent interval: $X^2 = 2.2$ (2), $P = 0.33$, Kruskal-Wallis ANOVA; naïve = 13 cells; unpaired = 10 cells; paired = 12 cells. **$P < 0.01$, Tukey's post hoc test. Box plots represent the median (center line), mean (square), quartiles, and 10-90% range (whiskers). Open circles represent data points for individual cells.

Figure 3. DP signals cue-related activity during fear memory acquisition and retrieval. (A) WT mice (n = 9) received infusions of a vector encoding GCaMP8f along with imaging fiber implantation directed at the DP. CS calcium-associated activity was monitored before, during, and after conditioning, in addition to after extinction. Fear conditioning consisted of a baseline period (300 s) followed by 6 pairings of CS (2 kHz, 20 s, 80 dB) and US (2 s, 0.7 mA). Pre-conditioning tone exposure, fear memory retrieval, and extinction memory retrieval all consisted of a baseline period (100 s) followed by four CS presentations (2 kHz, 20 s, 80 dB). (B) Representative histological image of GCaMP8f expression and fiber placement. Scale bar = 500 µm. (C) Left, raw calcium traces averaged across CS trials for each behavior test. Right, heat maps depicting individual calcium responses to each CS trial. (D) Comparison of $\Delta F/F$ percentage between pre- and post-conditioning CS presentation, as well as CS-associated activity following extinction training. $F_{2,15} = 17.7$, $P = 1.13 \times 10^{-4}$. **$P < 0.01$, Tukey's post hoc test. Box plots represent the median (center line), mean (square), quartiles, and 10-90% range (whiskers). Open circles represent data points for individual mice. Lines represent data points from the same animal.

Figure 4. Learning-activated DP neurons are reactivated following cue-evoked memory retrieval. (A) WT mice received infusions of a cocktail of vectors encoding ESARE-ERCreER-PEST, a conditional eYFP, and mCherry into the DP. After 4 weeks, mice were subjected to tones only (2 kHz, 20 s, 80 dB) or to paired presentations of CS (2 kHz, 20 s, 80 dB) and US (2 s, 0.7 mA) and immediately injected with vehicle or 4-OHT after training. Following 2 weeks, mice were subjected to a CS-evoked fear memory retrieval test or tone re-exposure in a neutral context. Mice were subjected to transcardial perfusion 90 min later and tissue was used to stain against cFos. (B) Representative histological image from brain sections of tone-exposed and conditioned mice injected with vehicle or 4-OHT. Scale bar = 500 µm. Inset and arrowheads indicate tagged neurons staining positive for cFos (red). Scale bar = 75 µm. Comparisons between tones-only vehicle (n = 4 mice, 8 slices), tones-only 4-OHT (n = 5 mice, 10 slices), conditioned vehicle (n = 4 mice, 8 slices), and conditioned 4-OHT (n = 6 mice, 12 slices) for (C) eYFP+ ($X^2 = 13.75$ (3), $P = 0.003$, Kruskal-Wallis ANOVA), (D) cFos+ ($F_{3,15} = 0.288$, $P = 0.83$, one-way ANOVA), (E) eYFP+ and cFos+ ($X^2 = 12.17$ (3), $P = 0.006$, Kruskal-Wallis ANOVA), and (F) eYFP+ and cFos+/ eYFP+ ($X^2 = 15.31$ (3), $P = 0.0016$, Kruskal-Wallis ANOVA). *$P < 0.05$, **$P < 0.01$, Tukey's post hoc test. Box plots represent the median (center line), mean (square), quartiles, and 10-90% range (whiskers). Open circles represent data points for individual mice.

Figure 5. DP neuron activity drives freezing and is necessary for fear memory expression. (A) WT mice received infusions of vectors encoding ESARE-ERCreER-PEST, conditional ChR2-eYFP or conditional Arch-GFP, and mCherry along with implantation of optical fibers directed at the DP. Mice were subjected to paired fear conditioning and immediately injected with either vehicle or 4-OHT. After 2 weeks, mice were subjected to a CS-evoked fear memory retrieval in a neutral context with and without optogenetic manipulation. (B) Freezing quantified during CS (2 kHz, 20 s, 80 dB) and light (473 nm, 20 Hz, 10 ms pulses, 20 s epochs) presentation for animals expressing ChR2 in fear-tagged DP neurons. Vehicle: $F_{3,15} = 22.14$, $P = 9.18 \times 10^{-6}$, one-way repeated-measures ANOVA; n = 6 mice. 4-OHT: $F_{3,15} = 73.39$, $P = 3.42 \times 10^{-9}$, one-way repeated-measures ANOVA; n = 6 mice. (C) Freezing quantified during CS (2 kHz, 20 s, 80 dB) and light (532 nm, solid light, 20 s epochs) presentation for animals expressing Arch in fear-tagged DP neurons. Vehicle: $F_{3,15} = 97.14$, $P = 4.73 \times 10^{-10}$, one-way repeated measures ANOVA; n = 6 mice. 4-OHT: $F_{3,15} = 53.29$, $P = 3.12 \times 10^{-8}$, one-way repeated measures ANOVA; n = 6 mice. **$P < 0.01$; ***$P < 0.001$ Tukey post hoc test. Box plots represent the median (center line), mean (square), quartiles, and 10-90% range (whiskers). Open circles represent data points for individual mice. Lines represent data points from the same animal.

References

1. Quirk, G.J., and Beer, J.S. (2006). Prefrontal involvement in the regulation of emotion: convergence of rat and human studies. Curr. Opin. Neurobiol. *16*, 723–727.

2. Sotres-Bayon, F., and Quirk, G.J. (2010). Prefrontal control of fear: more than just extinction. Curr. Opin. Neurobiol. *20*, 231–235.

3. Milad, M.R., and Quirk, G.J. (2012). Fear extinction as a model for translational neuroscience: ten years of progress. Annu. Rev. Psychol. *63*, 129–151.

4. Riga, D., Matos, M.R., Glas, A., Smit, A.B., Spijker, S., and Van den Oever, M.C. (2014). Optogenetic dissection of medial prefrontal cortex circuitry. Front. Syst. Neurosci. *8*, 230.

5. Do-Monte, F.H., Manzano-Nieves, G., Quiñones-Laracuente, K., Ramos-Medina, L., and Quirk, G.J. (2015). Revisiting the role of infralimbic cortex in fear extinction with optogenetics. J. Neurosci. *35*, 3607–3615.

6. Tang, J., Ko, S., Ding, H.-K., Qiu, C.-S., Calejesan, A.A., and Zhuo, M. (2005). Pavlovian fear memory induced by activation in the anterior cingulate cortex. Mol. Pain *1*, 6.

7. Bissière, S., Plachta, N., Hoyer, D., McAllister, K.H., Olpe, H.-R., Grace, A.A., and Cryan, J.F. (2008). The rostral anterior cingulate cortex modulates the efficiency of amygdala-dependent fear learning. Biol. Psychiatry *63*, 821–831.

8. Peters, J., Kalivas, P.W., and Quirk, G.J. (2009). Extinction circuits for fear and addiction overlap in prefrontal cortex. Learn. Mem. *16*, 279–288.

9. Kataoka, N., Shima, Y., Nakajima, K., and Nakamura, K. (2020). A central master driver of psychosocial stress responses in the rat. Science *367*, 1105–1112.

10. Nakamura, K., and Morrison, S.F. (2022). Central sympathetic network for thermoregulatory responses to psychological stress. Auton. Neurosci. *237*, 102918.

11. Nakamura, K., Nakamura, Y., and Kataoka, N. (2022). A hypothalamomedullary network for physiological responses to environmental stresses. Nat. Rev. Neurosci. *23*, 35–52.

12. Botterill, J.J., Khlaifia, A., Appings, R., Premachandran, H., Cruz-Sanchez, A., and Arruda-Carvalho, M. (2023). Dorsal peduncular cortex activity modulates affective behaviors in mice. bioRxiv, 2023.04.25.538301. 10.1101/2023.04.25.538301.

13. Phelps, E.A., Delgado, M.R., Nearing, K.I., and LeDoux, J.E. (2004). Extinction learning in humans: role of the amygdala and vmPFC. Neuron *43*, 897–905.

14. Schiller, D., Levy, I., Niv, Y., LeDoux, J.E., and Phelps, E.A. (2008). From fear to safety and back: reversal of fear in the human brain. J. Neurosci. *28*, 11517–11525.

15. Lanius, R.A., Williamson, P.C., Boksman, K., Densmore, M., Gupta, M., Neufeld, R.W.J., Gati, J.S., and Menon, R.S. (2002). Brain activation during script-driven imagery induced dissociative responses in PTSD: a functional magnetic resonance imaging investigation. Biol. Psychiatry *52*, 305–311.

16. Koenigs, M., Huey, E.D., Raymont, V., Cheon, B., Solomon, J., Wassermann, E.M., and Grafman, J. (2008). Focal brain damage protects against post-traumatic stress disorder in combat veterans. Nat. Neurosci. *11*, 232–237.

17. Cummings, K.A., Bayshtok, S., Dong, T.N., Kenny, P.J., and Clem, R.L. (2022). Control of fear by discrete prefrontal GABAergic populations encoding valence-specific information. Neuron. 10.1016/j.neuron.2022.07.004.

18. Kawashima, T., Kitamura, K., Suzuki, K., Nonaka, M., Kamijo, S., Takemoto-Kimura, S., Kano, M., Okuno, H., Ohki, K., and Bito, H. (2013). Functional labeling of neurons and their projections using the synthetic activity–dependent promoter E-SARE. Nat. Methods *10*, 889–895.

19. Morgan, M.A., and LeDoux, J.E. (1995). Differential contribution of dorsal and ventral medial prefrontal cortex to the acquisition and extinction of conditioned fear in rats. Behav. Neurosci. *109*, 681–688.

20. Morgan, M.A., Romanski, L.M., and LeDoux, J.E. (1993). Extinction of emotional learning: contribution of medial prefrontal cortex. Neurosci. Lett. *163*, 109–113.

21. Quirk, G.J., Russo, G.K., Barron, J.L., and Lebron, K. (2000). The role of ventromedial prefrontal cortex in the recovery of extinguished fear. J. Neurosci. *20*, 6225–6231.

22. Milad, M.R., and Quirk, G.J. (2002). Neurons in medial prefrontal cortex signal memory for fear extinction. Nature *420*, 70–74.

23. Vidal-Gonzalez, I., Vidal-Gonzalez, B., Rauch, S.L., and Quirk, G.J. (2006). Microstimulation reveals opposing influences of prelimbic and infralimbic cortex on the expression of conditioned fear. Learn. Mem. *13*, 728–733.

24. Sierra-Mercado, D., Padilla-Coreano, N., and Quirk, G.J. (2011). Dissociable roles of prelimbic and infralimbic cortices, ventral hippocampus, and basolateral amygdala in the expression and extinction of conditioned fear. Neuropsychopharmacology *36*, 529–538.

25. Sierra-Mercado, D., Jr, Corcoran, K.A., Lebrón-Milad, K., and Quirk, G.J. (2006). Inactivation of the ventromedial prefrontal cortex reduces expression of conditioned fear and impairs subsequent recall of extinction. Eur. J. Neurosci. *24*, 1751–1758.

26. Morgan, M.A., Schulkin, J., and LeDoux, J.E. (2003). Ventral medial prefrontal cortex and emotional perseveration: the memory for prior extinction training. Behav. Brain Res. *146*, 121–130.

563 27. Gewirtz, J.C., Falls, W.A., and Davis, M. (1997). Normal conditioned inhibition and extinction of freezing
564 and fear-potentiated startle following electrolytic lesions of medical prefrontal cortex in rats. Behav.
565 Neurosci. *111*, 712–726.

566 28. du Plessis, K.C., Basu, S., Rumbell, T.H., and Lucas, E.K. (2022). Sex-Specific Neural Networks of Cued
567 Threat Conditioning: A Pilot Study. Front. Syst. Neurosci. *16*, 832484.

568 29. Gretenkord, S., Rees, A., Whittington, M.A., Gartside, S.E., and LeBeau, F.E.N. (2017). Dorsal vs. ventral
569 differences in fast Up-state-associated oscillations in the medial prefrontal cortex of the urethane-
570 anesthetized rat. J. Neurophysiol. *117*, 1126–1142.

571 30. Oh, S.W., Harris, J.A., Ng, L., Winslow, B., Cain, N., Mihalas, S., Wang, Q., Lau, C., Kuan, L., Henry,
572 A.M., et al. (2014). A mesoscale connectome of the mouse brain. Nature *508*, 207–214.

573 31. Marek, R., Xu, L., Sullivan, R.K.P., and Sah, P. (2018). Excitatory connections between the prelimbic and
574 infralimbic medial prefrontal cortex show a role for the prelimbic cortex in fear extinction. Nat. Neurosci.
575 *21*, 654–658.

576 32. Cummings, K.A., and Clem, R.L. (2020). Prefrontal somatostatin interneurons encode fear memory. Nat.
577 Neurosci. *23*, 61–74.

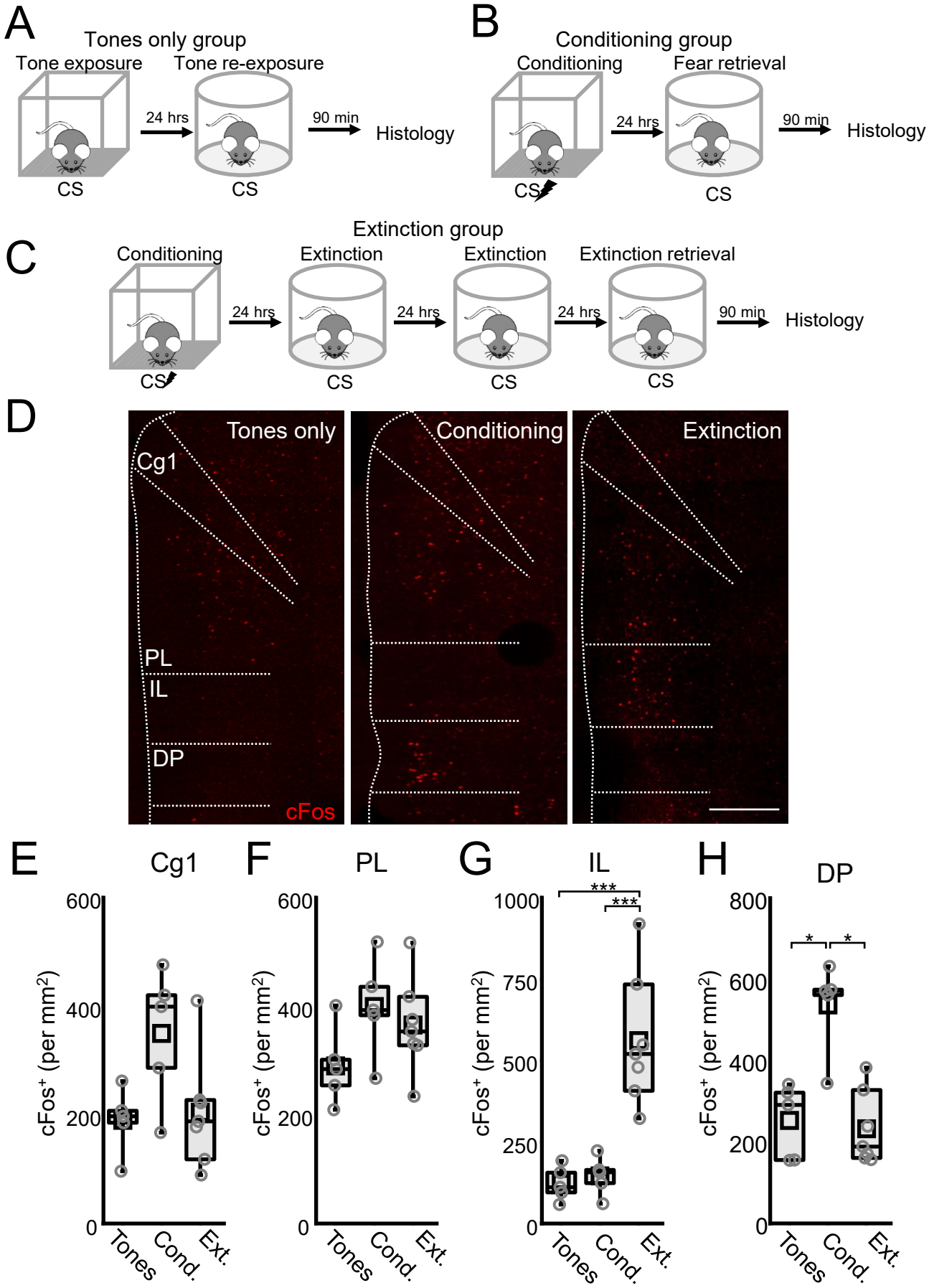

Figure 1. Fear conditioning drives activation of the DP. Mice were subjected either to (A) 6 tones (2 kHz, 20 s, 80 dB) followed by a tone re-exposure test consisting of 4 tone (2 kHz, 20 s, 80 dB) presentations 24 hours later; (B) paired presentations of a CS (2 kHz, 20 s, 80 dB) and US (2s, 0.7 mA) followed by a fear memory retrieval test consisting of 4 CS presentations (2 kHz, 20 s, 80 dB) 24 hours later; or to (C) paired presentations of a CS (2 kHz, 20 s, 80 dB) and US (2s, 0.7 mA) and 2 consecutive days of extinction training consisting of 20 CS (2 kHz, 20 s, 80 dB) presentations, and an extinction memory retrieval test consisting of 4 CS (2 kHz, 20 s, 80 dB) presentations. 90 minutes after tone re-exposure or fear or extinction memory retrieval, tissue was collected for cFos immunohistochemical analysis. (D) Representative histological images of prefrontal brain sections obtained from mice subjected to tones only, fear conditioning, or fear extinction. Scale = 500 µm. Comparisons of cFos+ puncta density between tones only (n = 5 mice, 10 slices), conditioning (n = 5 mice, 10 slices), and extinction (n = 7 mice, 14 slices) groups in the (E) anterior cingulate cortex 1 (Cg1: $F_{2,14} = 4.08$, P = 0.04, one-way ANOVA), (F) prelimbic cortex (PL: $F_{2,14} = 2.23$, P = 0.14, one-way ANOVA), (G) infralimbic cortex (IL: $F_{2,14} = 19.34$, P = 9.4 x 10^{-4}, one-way ANOVA), and (H) dorsal peduncular cortex (DP: $X^2 = 9.39$ (2), P = 0.009, Kruskal-Wallis ANOVA). *P < 0.05, ***P < 0.001, Tukey's post-hoc test. Box plots represent the median (center line), mean (square), quartiles, and 10-90% range (whiskers). Open circles represent data points for individual mice.

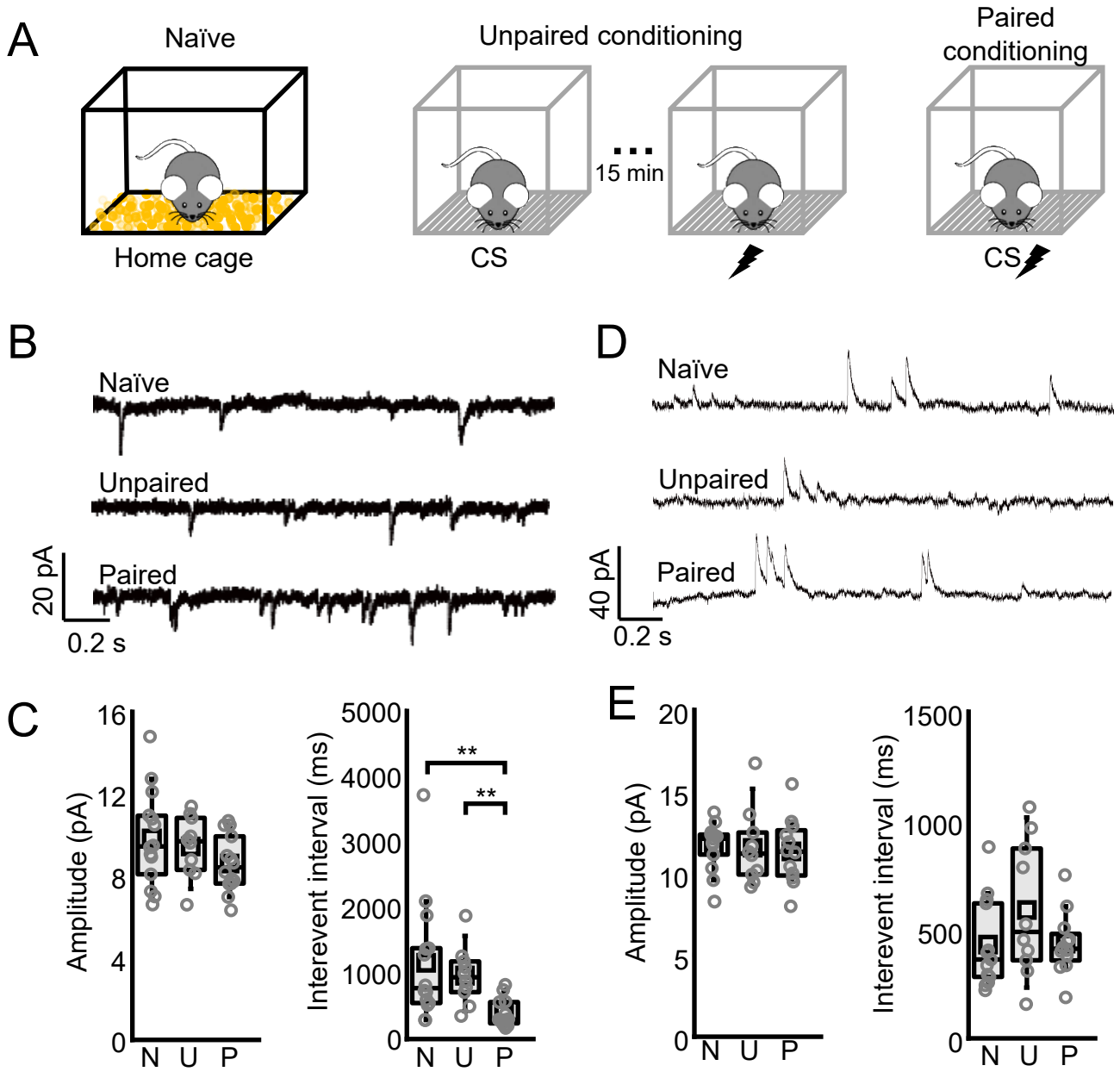

Figure 2. Fear conditioning drives increased glutamatergic transmission onto DP PNs. (A) Mice were either experienced to their home cage (naïve) or subjected to unpaired or paired presentations of a CS (2 kHz, 20 s, 80 dB) and US (2s, 1 mA). Whole-cell recordings were performed 24 hours after training. (B) Representative spontaneous excitatory postsynaptic current (EPSC) recordings in DP PNs from brain slices prepared from naïve (8 slices from 4 mice), unpaired (5 slices from 3 mice), and paired (8 slices from 4 mice) mice. (C) Quantification of the EPSC amplitude and interevent interval for naïve, unpaired, and paired groups. Amplitude: $F_{2,35} = 1.67$, $P = 0.2$, one-way ANOVA; naïve = 14 cells; unpaired = 10 cells; paired = 14 cells. Interevent interval: $X^2 = 14.32$ (2), $P = 7.77 \times 10^{-4}$, Kruskal-Wallis ANOVA; naïve = 14 cells; unpaired = 10 cells; paired = 14 cells. (D) Representative spontaneous inhibitory postsynaptic current (IPSC) recordings in DP PNs from brain slices prepared from naïve, unpaired, and paired mice. (E) Quantification of the IPSC amplitude and interevent interval for naïve, unpaired, and paired groups. Amplitude: $F_{2,32} = 0.084$, $P = 0.92$, one-way ANOVA; naïve = 13 cells; unpaired = 10 cells; paired = 12 cells. Interevent interval: $X^2 = 2.2$ (2), $P = 0.33$, Kruskal-Wallis ANOVA; naïve = 13 cells; unpaired = 10 cells; paired = 12 cells. **$P < 0.01$, Tukey's post hoc test. Box plots represent the median (center line), mean (square), quartiles, and 10-90% range (whiskers). Open circles represent data points for individual cells.

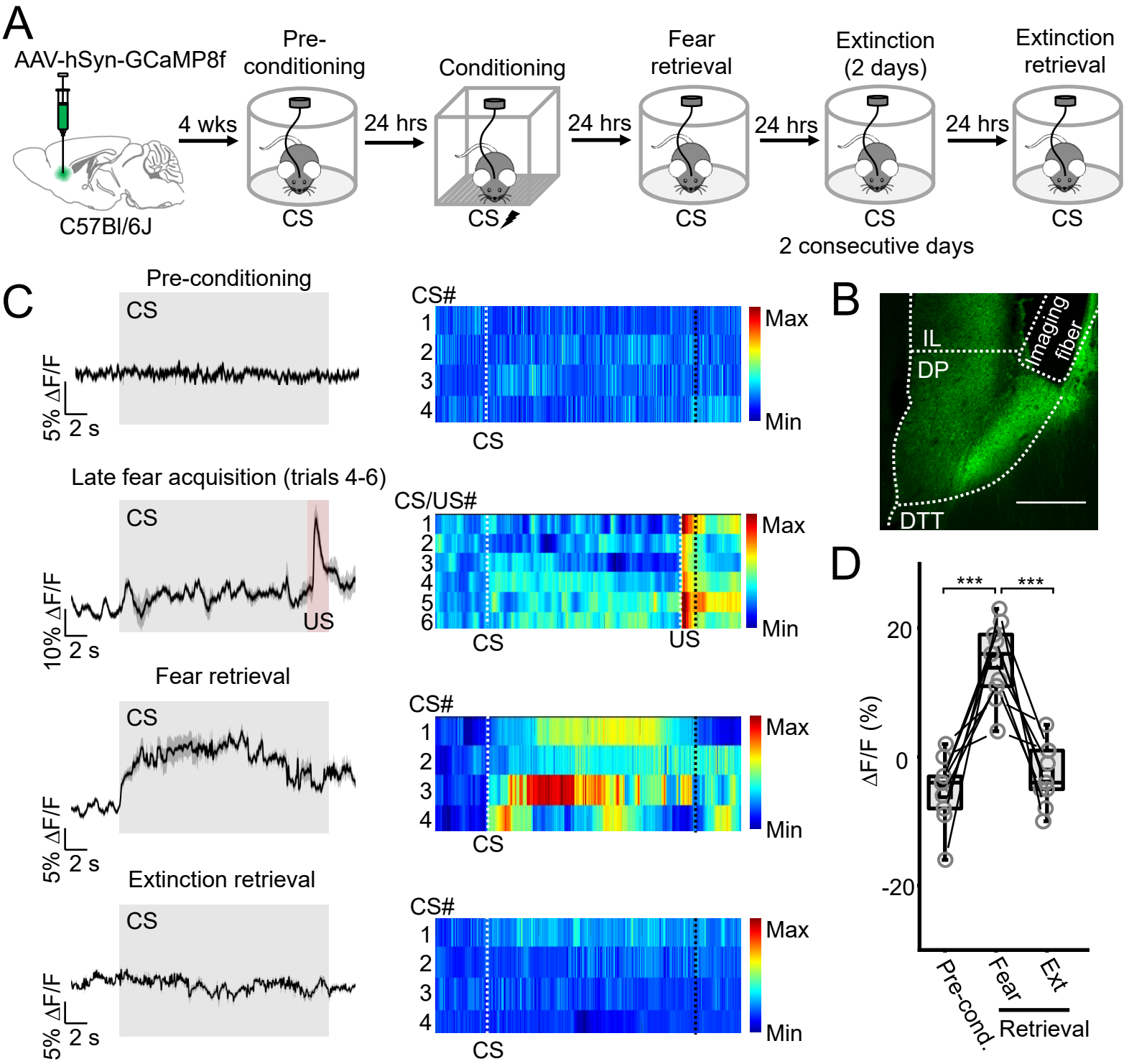

Figure 3. DP signals cue-related activity during fear memory acquisition and retrieval. (A) WT mice (n = 9) received infusions of a vector encoding GCaMP8f along with imaging fiber implantation directed at the DP. CS calcium-associated activity was monitored before, during, and after conditioning, in addition to after extinction. Fear conditioning consisted of a baseline period (300 s) followed by 6 pairings of CS (2 kHz, 20 s, 80 dB) and US (2 s, 0.7 mA). Pre-conditioning tone exposure, fear memory retrieval, and extinction memory retrieval all consisted of a baseline period (100 s) followed by four CS presentations (2 kHz, 20 s, 80 dB). (B) Representative histological image of GCaMP8f expression and fiber placement. Scale bar = 500 µm. (C) Left, raw calcium traces averaged across CS trials for each behavior test. Right, heat maps depicting individual calcium responses to each CS trial. (D) Comparison of ΔF/F percentage between pre- and post-conditioning CS presentation, as well as CS-associated activity following extinction training. $F_{2,15} = 17.7$, $P = 1.13 \times 10^{-4}$. **P < 0.01, Tukey's post hoc test. Box plots represent the median (center line), mean (square), quartiles, and 10-90% range (whiskers). Open circles represent data points for individual mice. Lines represent data points from the same animal.

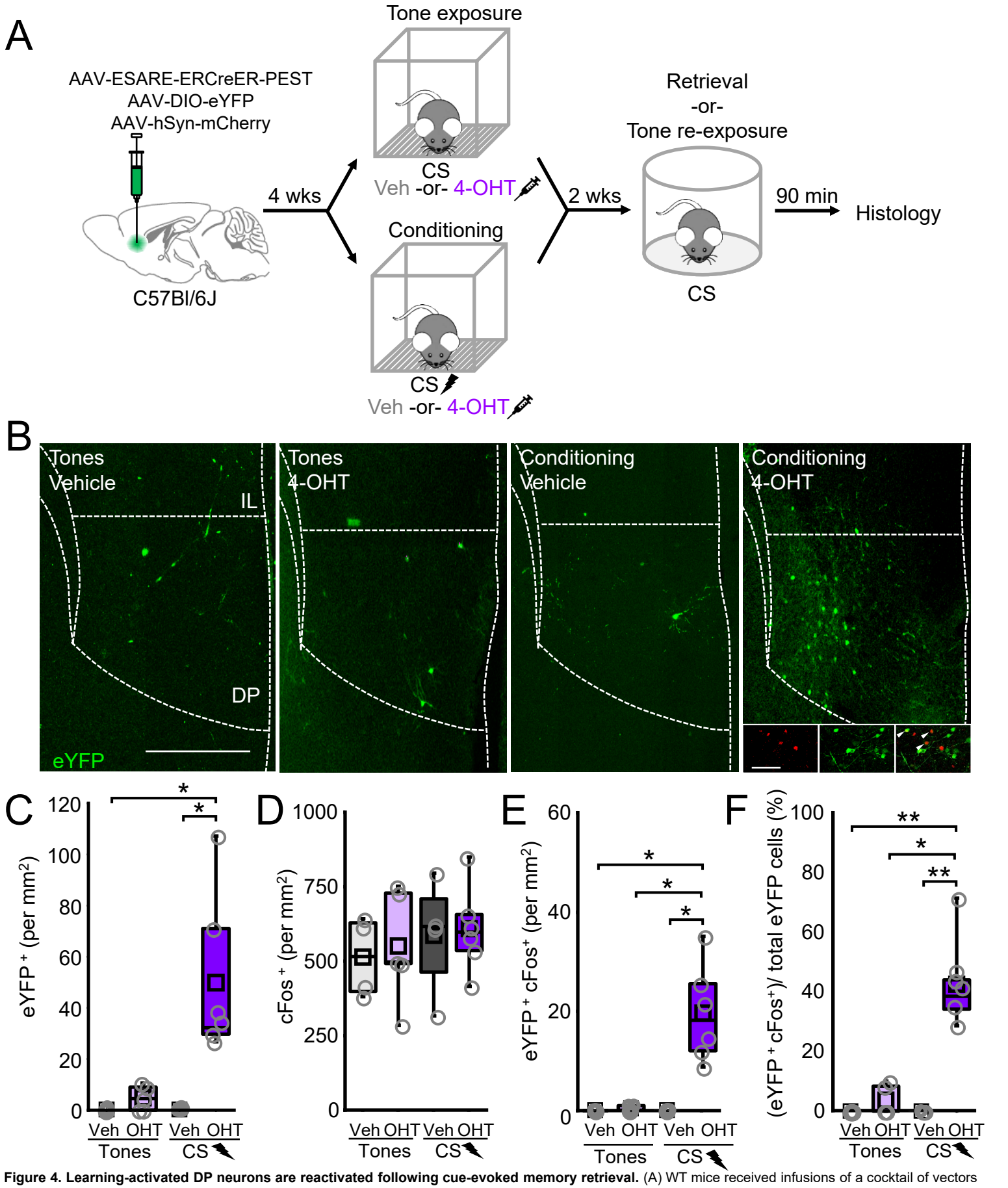

Figure 4. Learning-activated DP neurons are reactivated following cue-evoked memory retrieval. (A) WT mice received infusions of a cocktail of vectors encoding ESARE-ERCreER-PEST, a conditional eYFP, and mCherry into the DP. After 4 weeks, mice were subjected to tones only (2 kHz, 20 s, 80 dB) or to paired presentations of CS (2 kHz, 20 s, 80 dB) and US (2 s, 0.7 mA) and immediately injected with vehicle or 4-OHT after training. Following 2 weeks, mice were subjected to a CS-evoked fear memory retrieval test or tone re-exposure in a neutral context. Mice were subjected to transcardial perfusion 90 min later and tissue was used to stain against cFos. (B) Representative histological image from brain sections of tone-exposed and conditioned mice injected with vehicle or 4-OHT. Scale bar = 500 µm. Inset and arrowheads indicate tagged neurons staining positive for cFos (red). Scale bar = 75 µm. Comparisons between tones-only vehicle (n = 4 mice, 8 slices), tones-only 4-OHT (n = 5 mice, 10 slices), conditioned vehicle (n = 4 mice, 8 slices), and conditioned 4-OHT (n = 6 mice, 12 slices) for (C) eYFP+ (X^2 = 13.75 (3), P = 0.003, Kruskal-Wallis ANOVA), (D) cFos+ ($F_{3,15}$ = 0.288, P = 0.83, one-way ANOVA), (E) eYFP+ and cFos+ (X^2 = 12.17 (3), P = 0.006, Kruskal-Wallis ANOVA), and (F) eYFP+ and cFos+/ eYFP+ (X^2 = 15.31 (3), P = 0.0016, Kruskal-Wallis ANOVA). *P < 0.05, **P < 0.01, Tukey's post hoc test. Box plots represent the median (center line), mean (square), quartiles, and 10-90% range (whiskers). Open circles represent data points for individual mice.

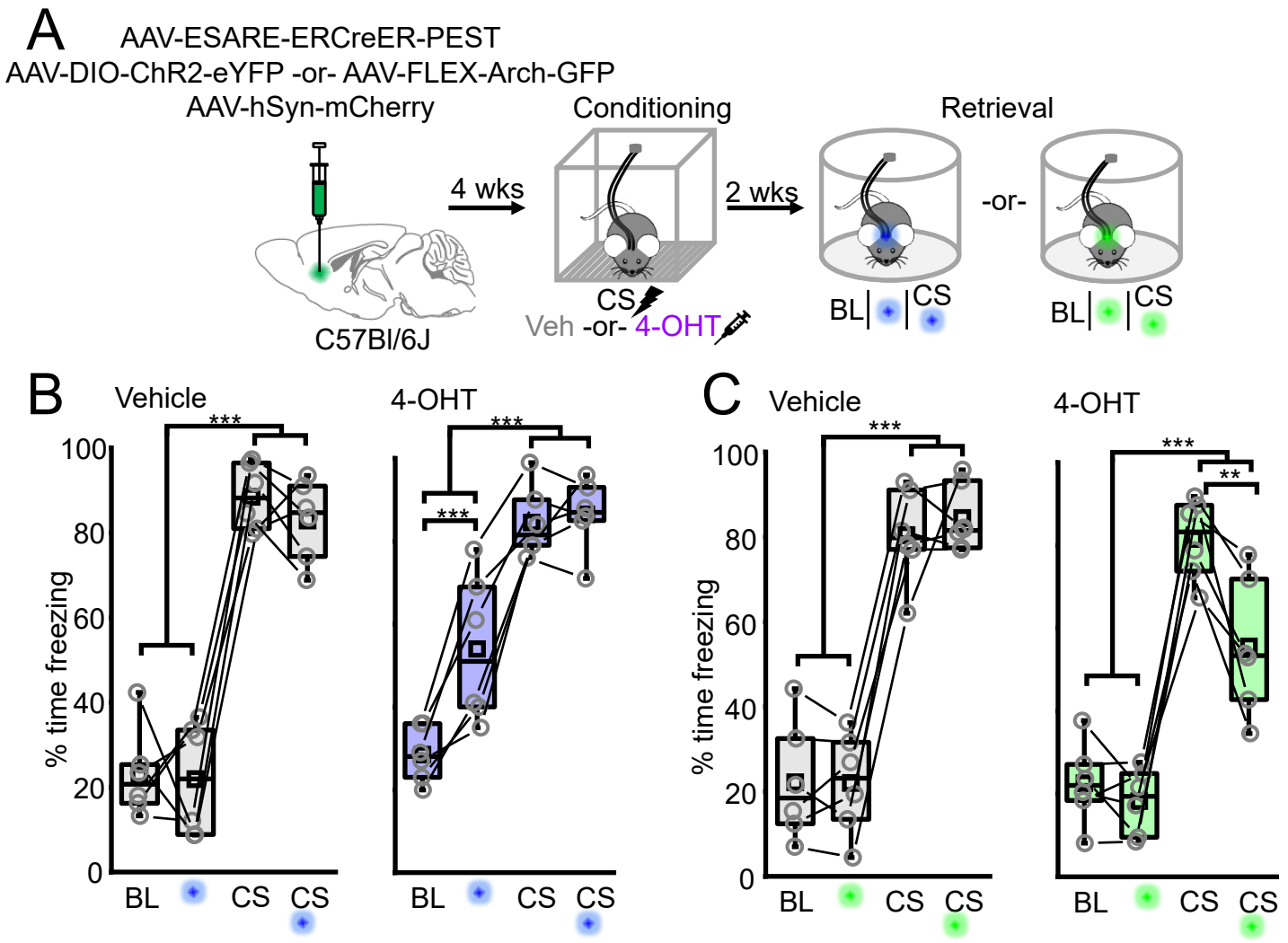

Figure 5. DP neuron activity drives freezing and is necessary for fear memory expression. (A) WT mice received infusions of vectors encoding ESARE-ERCreER-PEST, conditional ChR2-eYFP or conditional Arch-GFP, and mCherry along with implantation of optical fibers directed at the DP. Mice were subjected to paired fear conditioning and immediately injected with either vehicle or 4-OHT. After 2 weeks, mice were subjected to a CS-evoked fear memory retrieval in a neutral context with and without optogenetic manipulation. (B) Freezing quantified during CS (2 kHz, 20 s, 80 dB) and light (473 nm, 20 Hz, 10 ms pulses, 20 s epochs) presentation for animals expressing ChR2 in fear-tagged DP neurons. Vehicle: $F_{3,15} = 22.14$, $P = 9.18 \times 10^{-6}$, one-way repeated-measures ANOVA; n = 6 mice. 4-OHT: $F_{3,15} = 73.39$, $P = 3.42 \times 10^{-9}$, one-way repeated-measures ANOVA; n = 6 mice. (C) Freezing quantified during CS (2 kHz, 20 s, 80 dB) and light (532 nm, solid light, 20 s epochs) presentation for animals expressing Arch in fear-tagged DP neurons. Vehicle: $F_{3,15} = 97.14$, $P = 4.73 \times 10^{-10}$, one-way repeated measures ANOVA; n = 6 mice. 4-OHT: $F_{3,15} = 53.29$, $P = 3.12 \times 10^{-8}$, one-way repeated measures ANOVA; n = 6 mice. **P < 0.01; ***P < 0.001 Tukey post hoc test. Box plots represent the median (center line), mean (square), quartiles, and 10-90% range (whiskers). Open circles represent data points for individual mice. Lines represent data points from the same animal.

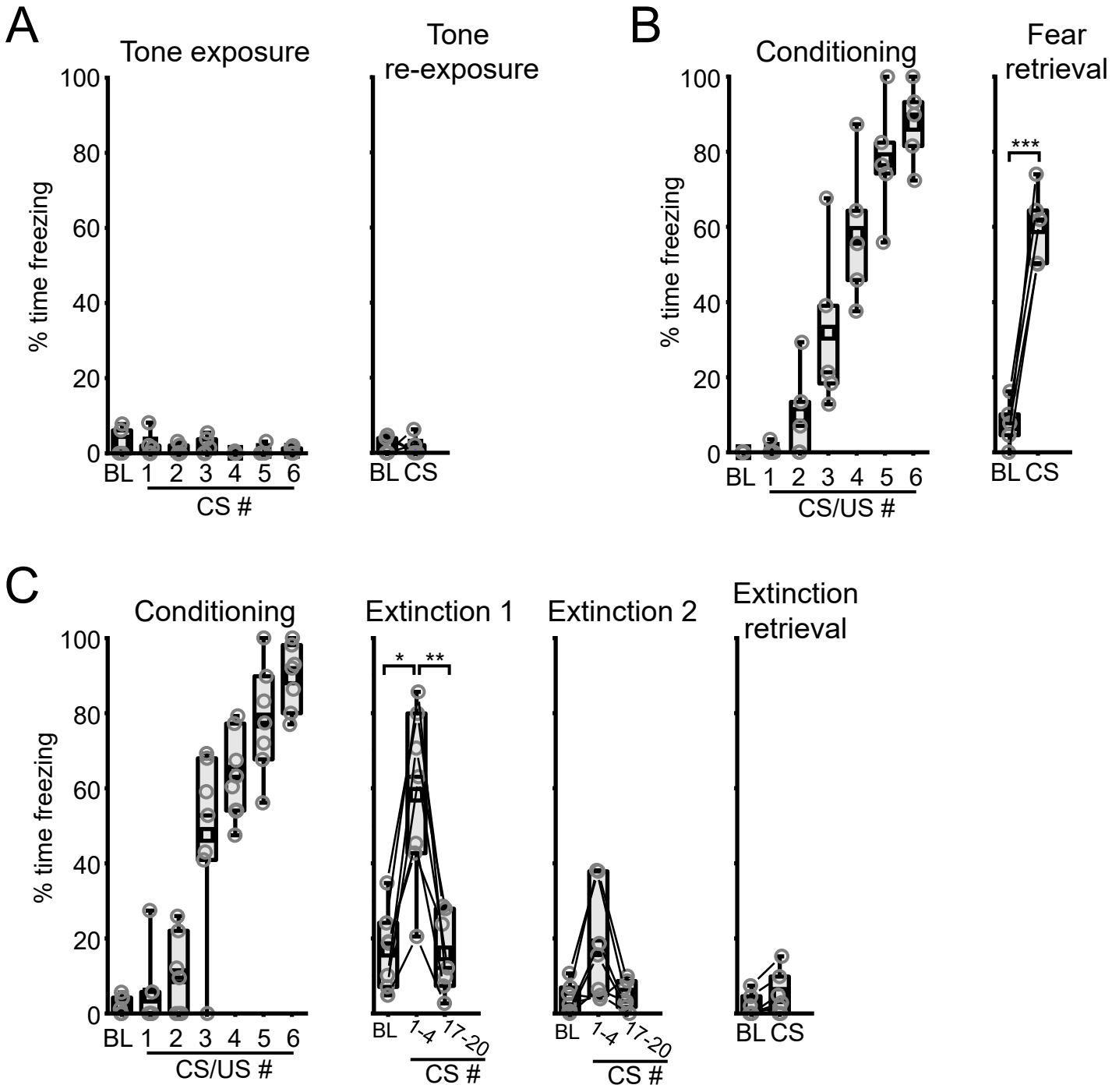

Supplementary Figure 1. Behavior analysis for mice used for cFos immunohistochemistry. (A) Quantification of freezing for mice subjected to tone exposure and tone re-exposure (W = 5, P = 1, Wilcoxen signed rank test). (B) Quantification of freezing for mice that were fear conditioned and subjected to fear memory retrieval (t(4) = -11.52, P = 3.24 x 10-4, Paired t-test). (C) Quantification of freezing for mice that were fear conditioned and subjected to a first day of extinction training (X^2 (2) = 10.57, P = 0.005, Friedman ANOVA), a second day of extinction training (X^2(2) = 5.43, P = 0.066, Friedman ANOVA), and extinction memory retrieval (W = 2, P = 0.094, Wilcoxen signed rank test). *, P < 0.05, **, P < 0.01, Dunn's post-hoc test. Box plots represent the median (center line), mean (square), quartiles, and 10-90% range (whiskers). Open circles represent data points for individual mice.

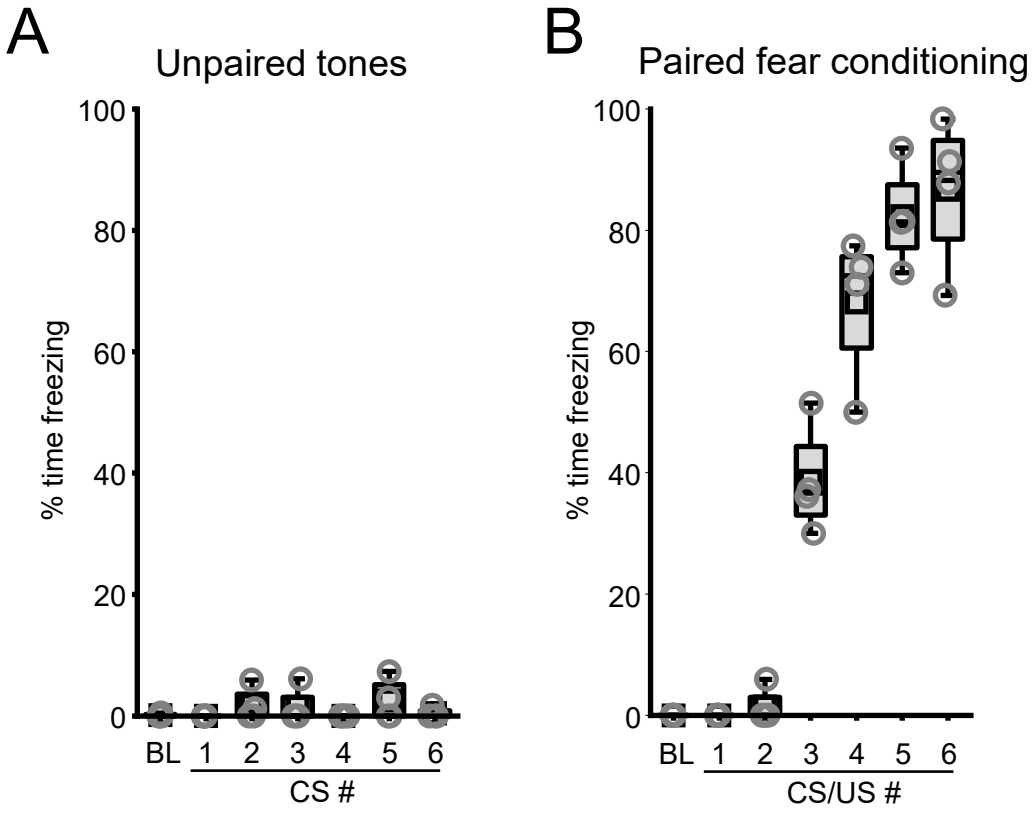

Supplementary Figure 2. Behavior analysis for mice used for electrophysiology recordings. (A) Quantification of freezing during unpaired tone presentation. (B) Quantification of freezing during paired fear conditioning. Box plots represent the median (center line), mean (square), quartiles, and 10-90% range (whiskers). Open circles represent data points for individual mice.

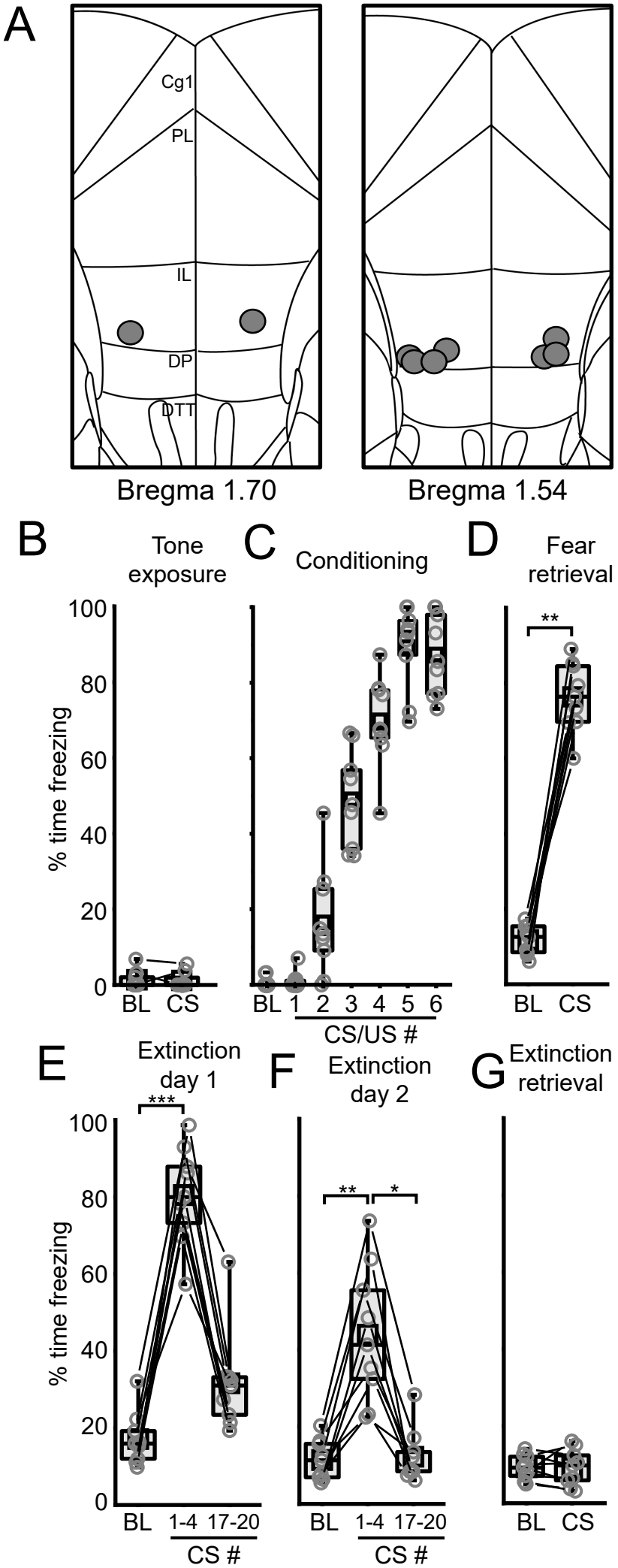

Supplementary Figure 3. Fiber photometry fiber placements and behavioral data. (A) Fiber placements. Gray circles represent imaging fiber tip termination positions. Quantification of percent time freezing during (B) tone exposure, W = 3, P = 1, Wilcoxen signed rank test, (C) fear conditioning, (D) fear memory retrieval, W = 0, P = 0.004, Wilcoxen signed rank test, (E) extinction day 1, X^2 (2) = 18, Friedman ANOVA, (F) extinction day 2, X^2 (2) = 14, Friedman ANOVA, and (G) extinction memory retrieval, t(8) = 0.069, P = 0.95, paired t-test. *, P < 0.05, **, P < 0.01, ***, P < 0.001, Dunn's post-hoc test. Box plots represent the median (center line), mean (square), quartiles, and 10-90% range (whiskers). Open circles represent data points for individual mice. Lines represent data points from the same animal.

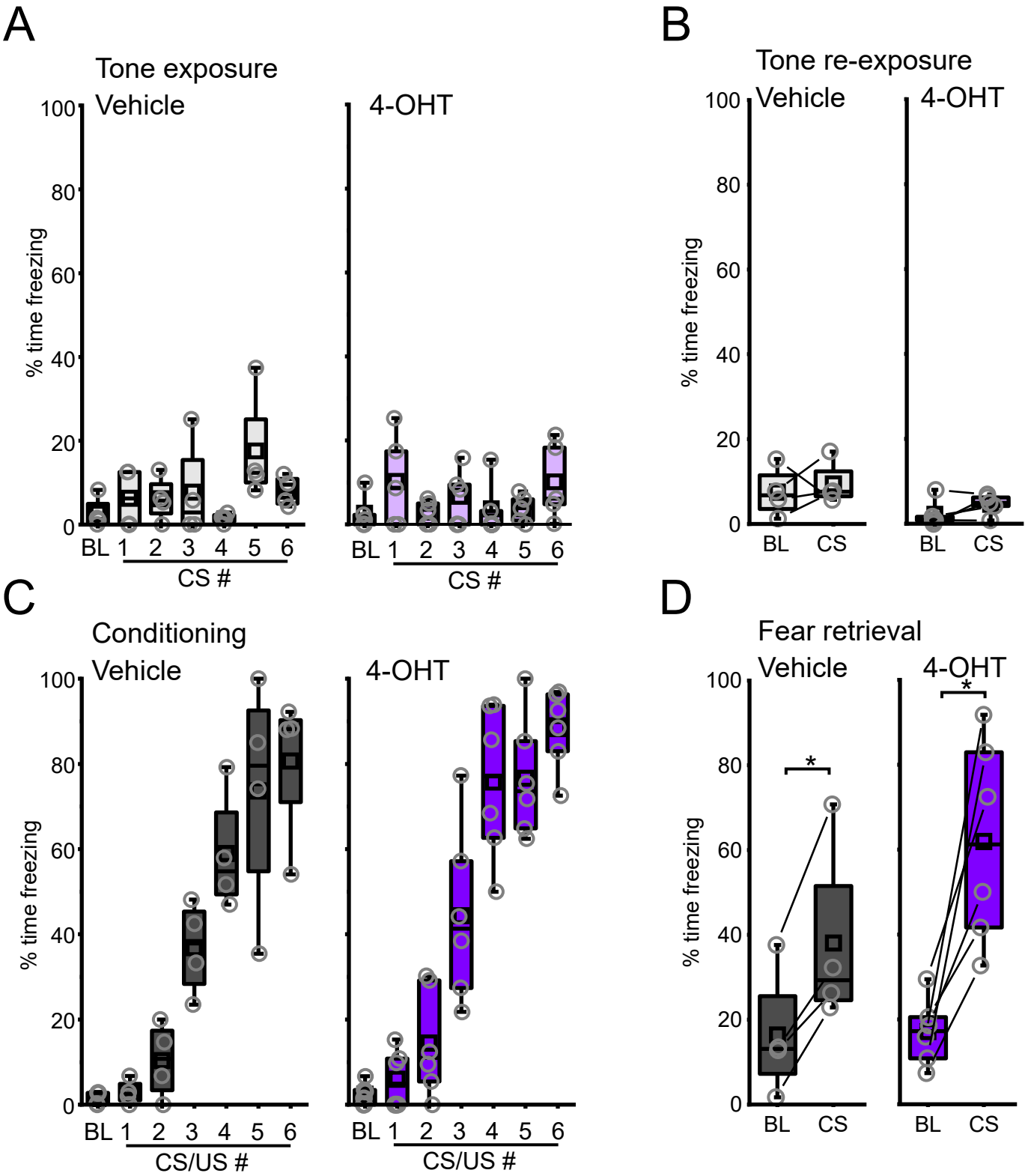

Supplementary Figure 4. Behavior analysis associated with neural tagging data. Quantification of freezing during (A) tone exposure and (B) tone re-exposure (vehicle: t(3) = -0.48, P = 0.67, paired t-test; 4-OHT: W = 3, P = 0.31, Wilcoxen signed rank test). Quantification of freezing during (C) fear conditioning and (B) fear memory retrieval (vehicle: t(3) = -5.23, P = 0.014, paired t-test; 4-OHT: W = 0, P = 0.03, Wilcoxen signed rank test). Box plots represent the median (center line), mean (square), quartiles, and 10-90% range (whiskers). Open circles represent data points for individual mice.

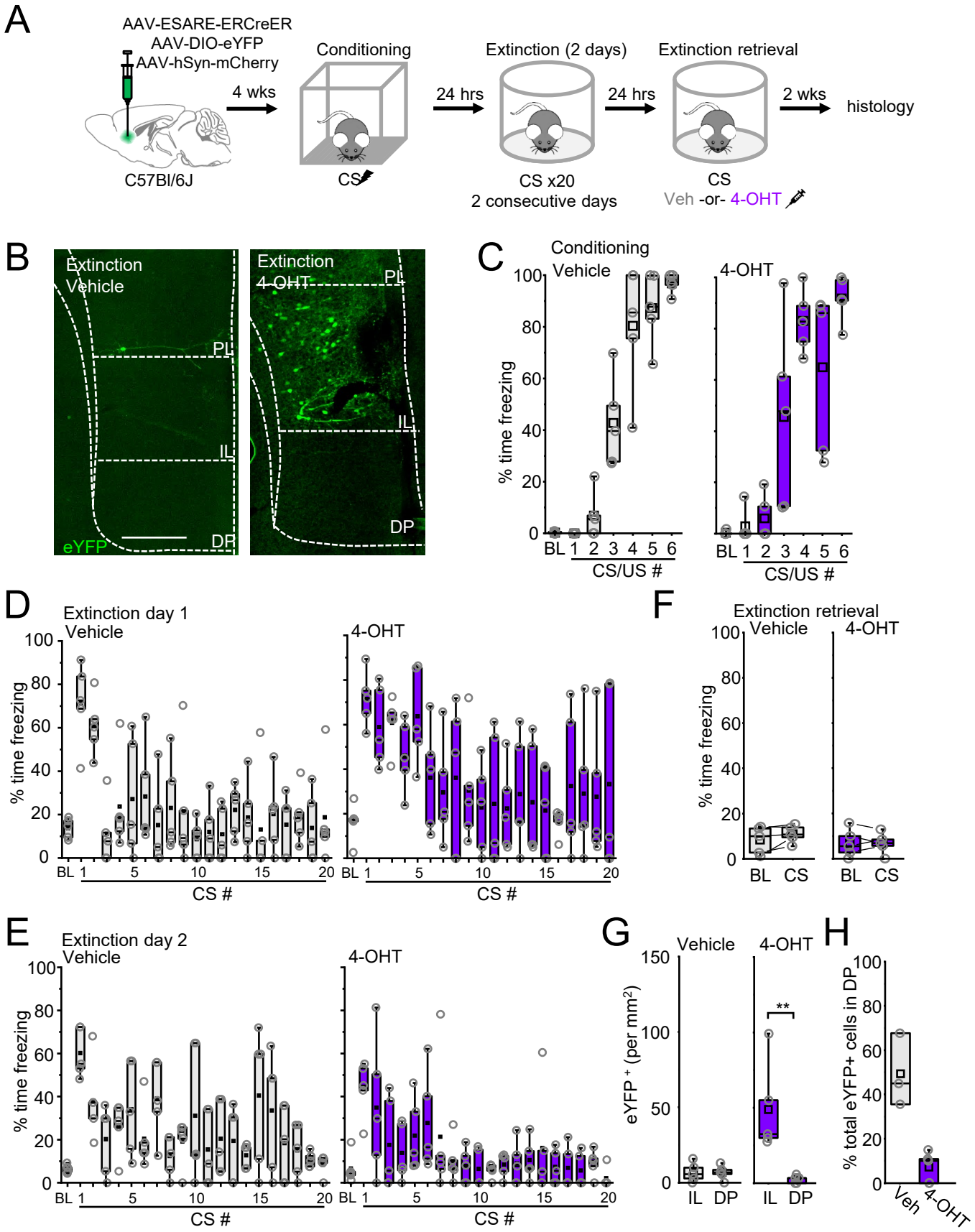

Supplementary Figure 5. Behavior analysis and histology for neural tagging in response to extinction training. (A) Behavioral paradigm for tagging infralimbic (IL) and dorsal peduncular (DP) cortex neurons following extinction training. (B) Representative histological images for animals subjected to extinction training and injected with either vehicle or 4-hydroxytamoxifen (4-OHT). Scale bar = 500 µm. Quantification of freezing during (C) fear conditioning, (D) day 1 of extinction training, (E) day 2 of extinction training, and (F) extinction memory retrieval (vehicle: $t(4) = -1.81$, $P = 0.14$, paired t-test; 4-OHT: $t(4) = 0.02$, $P = 0.99$, paired t-test). (G) Quantification of the number eYFP+ neurons in the IL and DP (vehicle: $t(8) = 0.008$, $P = 0.99$, two-sample t-test; 4-OHT: $U = 25$, $P = 0.012$, Mann-Whitney U-test). (H) Quantification of the fraction of total eYFP+ neurons that are localized in the DP ($t(6) = -5.24$, $P = 0.002$, two-sample t-test). Box plots represent the median (center line), mean (square), quartiles, and 10-90% range (whiskers). Open circles represent data points for individual mice.

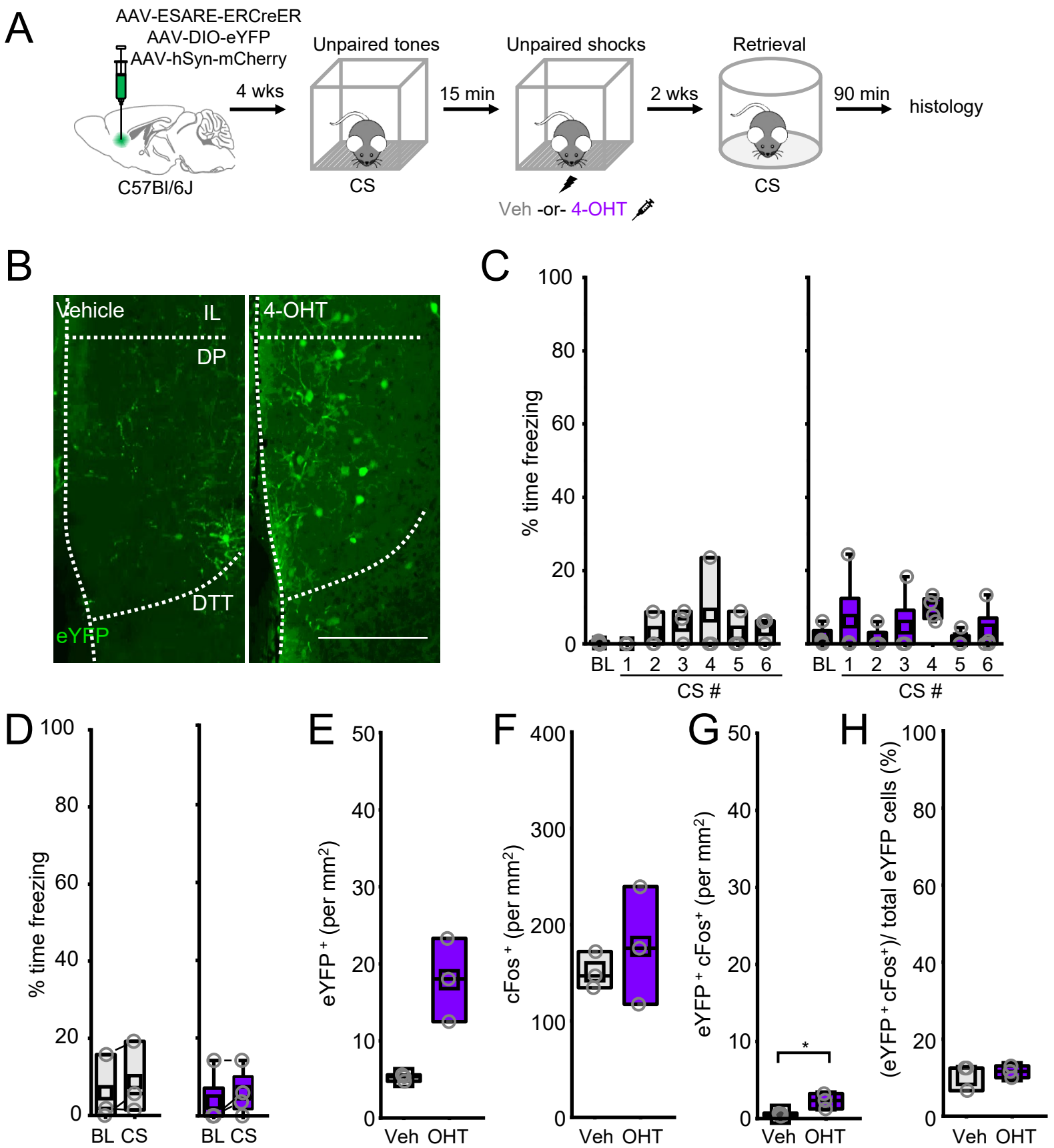

Supplementary Figure 6. Behavior analysis and histology for neural tagging in response to unpaired conditioning. (A) Four weeks after vector infusion, mice were subjected to unpaired fear conditioning and injected with vehicle or 4-OHT immediately after shock delivery. Following 2 weeks, mice were subjected to a CS-evoked fear memory retrieval test and tissue was processed for cFos staining 90 minutes later. (B) Representative histological images from vehicle- and 4-OHT-injected mice. Scale bar = 500 µm. (C) Quantification of the percent time freezing during unpaired CS presentation for vehicle (gray) and 4-OHT (purple) mice. (D) Quantification of the percent time freezing during CS-evoked fear memory test for vehicle ($t(2) = -1.63$, $P = 0.25$, paired t-test) and 4-OHT ($W = 0$, $P = 0.25$, Wilcoxen signed-rank test). Comparisons between unpaired vehicle (n = 4 mice) and unpaired 4-OHT mice (n = 3) for (E) eYFP+ ($U = 0$, $P = 0.081$, Mann-Whitney U test), (F) cFos+ ($t(4) = -0.71$, $P = 0.52$), (G) eYFP+ and cFos+ ($t(4) = -2.96$, $P = 0.041$), and (H) eYFP+ and cFos+/ eYFP+ ($U = 4$, $P = 1$, Mann-Whitney U-test). Box plots represent the median (center line), mean (square), quartiles, and 10-90% range (whiskers). Open circles represent data points for individual mice.

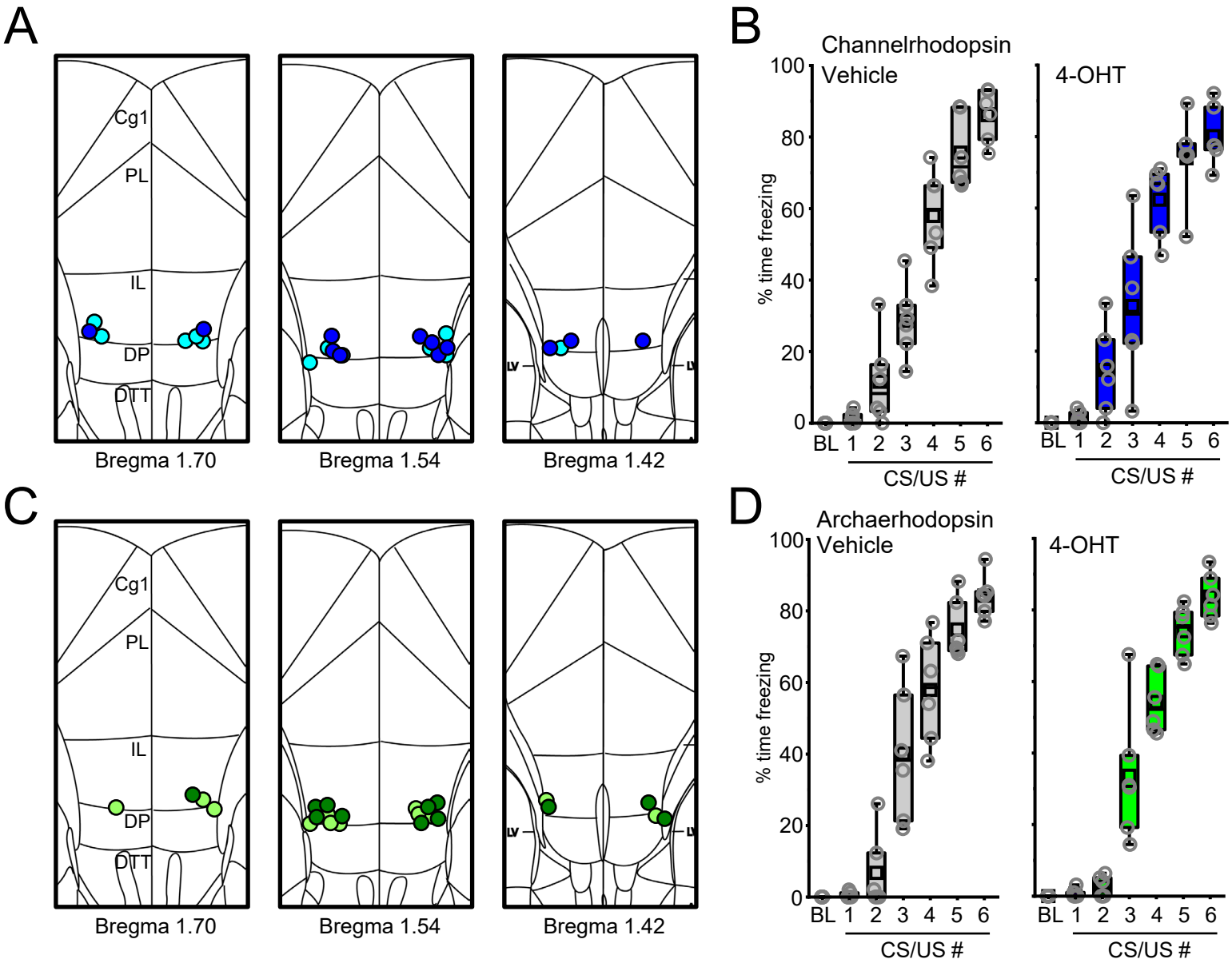

Supplementary figure 7. Fiber placements and behavioral data for optogenetic experiments. (A) Optic fiber placements for channelrhodopsin-expressing mice. Light blue and dark blue circles represent optic fiber tip termination positions for vehicle- and 4-OHT-injected mice, respectively. (B) Quantification of percent time freezing during fear conditioning for vehicle- (gray) and 4-OHT- (blue) injected channelrhodopsin-expressing mice. (C) Optic fiber placements for archaerhodopsin-expressing mice. Light green and dark green circles represent optic fiber tip termination positions for vehicle- and 4-OHT-injected mice, respectively. (D) Quantification of percent time freezing during fear conditioning for vehicle- (gray) and 4-OHT- (green) injected archaerhodopsin-expressing mice. Box plots represent the median (center line), mean (square), quartiles, and 10-90% range (whiskers). Open circles represent data points for individual mice.

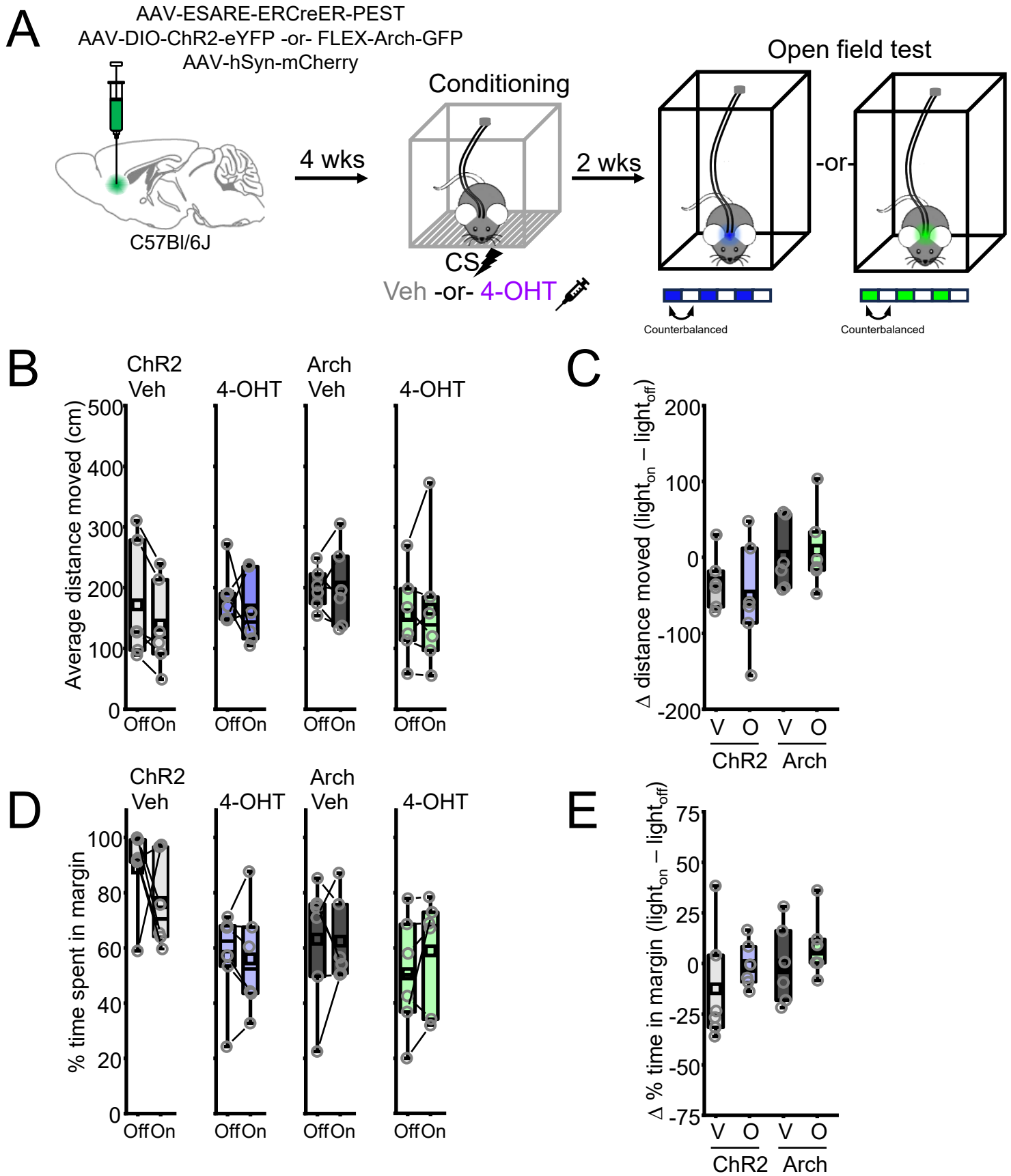

Supplementary figure 8. Optogenetic manipulations during the open field test. (A) Neural tagging and manipulation paradigm. Four weeks after vector infusion and optic fiber implantation, mice were subjected to paired fear conditioning and injected with vehicle or 4-OHT immediately after. Following 2 weeks, mice were placed in an open field for 10 minutes and optogenetic activation (for ChR2-injected mice: 473 nm, 20 Hz, 5 ms pulses, 1 min on/off epochs) or silencing (for Arch-injected mice: 532 nm, solid light, 1 min on/off epochs) was performed. (B) Quantification of distance moved during light on and light off epochs for vehicle- ($t(5) = 2.23$, $P = 0.076$, paired t-test) and 4-OHT- ($t(5) = 0.62$, $P = 0.56$, paired t-test) injected ChR2 mice and vehicle- ($t(5) = -0.09$, $P = 0.93$, paired t-test) and 4-OHT- ($t(5) = -0.43$, $P = 0.69$, paired t-test). (C) Quantification of the change in distance moved was performed by subtracting distance during light_on from light_off ($F(3) = 1.71$, $P = 0.2$). V is vehicle, O is 4-OHT. (D) Quantification of the percent time spent in the open field margin during light on and light off epochs for vehicle- ($W = 14$, $P = 0.56$, Wilcoxen signed-rank test) and 4-OHT- ($t(5) = 0.2$, $P = 0.85$, paired t-test) injected ChR2 mice and vehicle- ($t(5) = 0.09$, $P = 0.93$, paired t-test) and 4-OHT- ($t(5) = -1.32$, $P = 0.24$, paired t-test). (E) Quantification of the change in the percent time spent in the margin was performed by subtracting percent time in margin during light_on from light_off ($F(3) = 1.11$, $P = 0.37$, one-way ANOVA). V is vehicle, O is 4-OHT. Box plots represent the median (center line), mean (square), quartiles, and 10-90% range (whiskers). Open circles represent data points for individual mice.

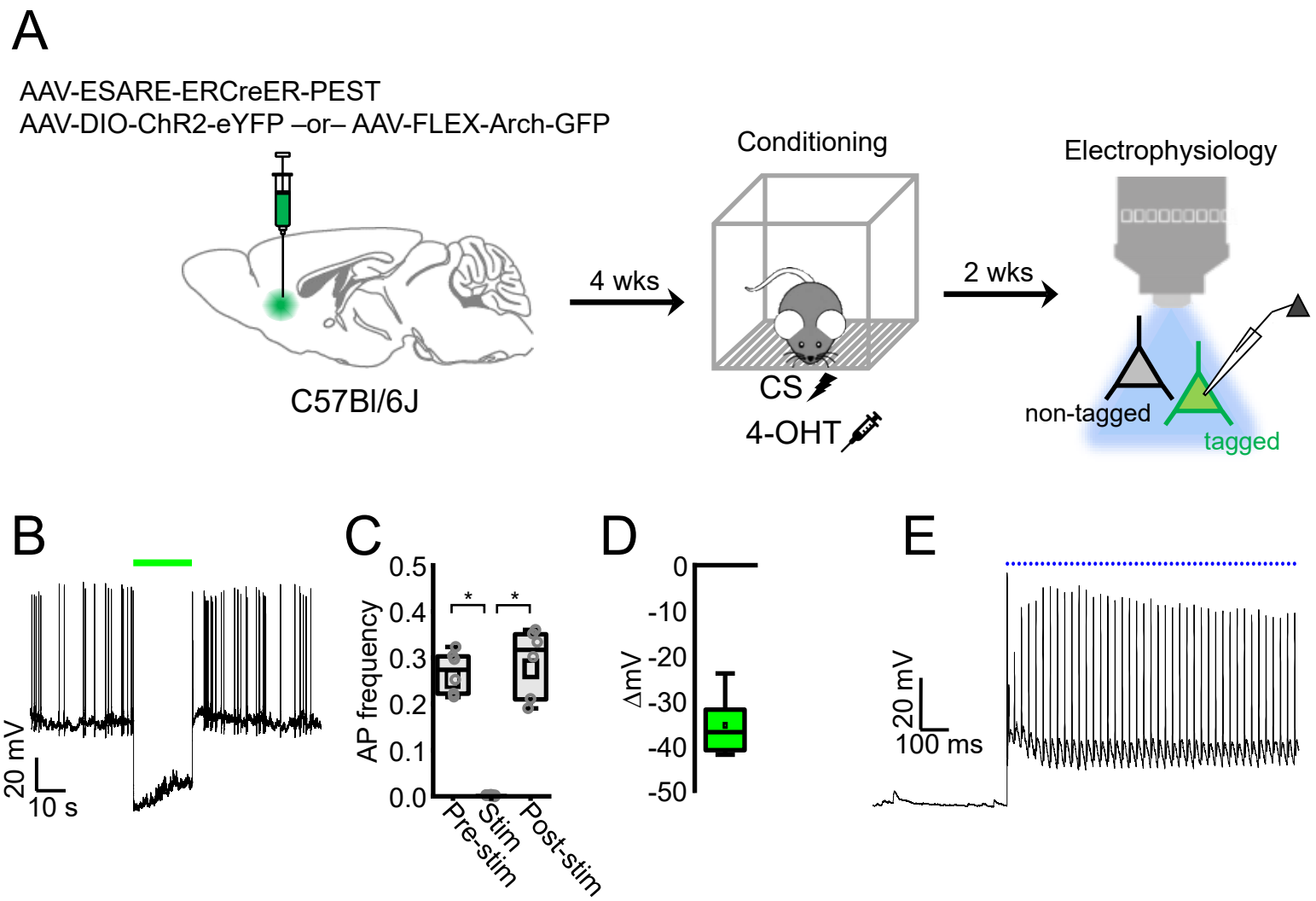

Supplementary figure 9. Electrophysiological validation of optogenetic manipulations. (A) ESARE-ERCreER and a Cre-dependent ChR2-eYFP or Cre-dependent Arch-GFP was infused into the DP of wild-type male and female mice. Mice were subjected to paired fear conditioning 4 weeks later and immediately injected with 4-OHT after training. After 2 weeks, acute brain slices were prepared and recordings were made from ChR2- or Arch-expressing fear-tagged DP neurons. (B) Example recording of spontaneous action potential firing from a neuron expressing Arch with and without optogenetic silencing (532 nm; solid light, 20 s epoch; denoted with green line). (C) Quantification of spontaneous action potential firing before, during, and after optogenetic silencing. X^2 (2) = 0.009, Friedman ANOVA. n = 6 cells from 3 mice. (D) Quantification of the change in steady-state membrane potential during optogenetic silencing compared to a pre-stim baseline. n = 6 cells from 3 mice. (E) Representative recording of action potentials elicited by pulses of blue light (473 nm; 20 Hz, 5 ms pulses, 20 s epochs) in ChR2-expressing tagged neurons. n = 8 cells from 3 mice. *, $P < 0.05$, Dunn's post-hoc test. Box plots represent the median (center line), mean (square), quartiles, and 10-90% range (whiskers). Open circles represent data points for individual cells.